ARCHIVES OF ACOUSTICS
7, 1, 3–12 (1982)

PERCEPTIBILITY OF PITCH CHANGES IN A TONAL SIGNAL EMITTED BY A MOVING SOURCE

URSZULA JORASZ

Department of Acoustics, Adam Mickiewicz University (60-769 Poznań, ul. Matejki 48/49)

The starting point for the experimental research described here was a psychoacoustic analysis of the Doppler effect. The investigations were performed under laboratory conditions using an electronic model of a moving source. Data were obtained on the relationship between the sensations of pitch and loudness of a tonal signal under dynamic conditions.

1. Introduction

The starting point for the experimental research was a psychoacoustic analysis of the Doppler effect in the case of a tonal signal. The experimental investigations consisted in the considerations of the perceptibility by a static observer of a signal emitted by a moving source. This signal was characterized by a simultaneous change in its two physical parameters: frequency and intensity. Both quantities were also variable in time.

Analysis of the Doppler effect can, therefore, be reduced to the investigation of the perceptibility of pitch changes in a signal under the conditions of a simultaneous change in its loudness.

It can be assumed that the frequency f_0 of a tone emitted by a static source with respect to the observer is 1000 Hz. It can also be assumed in terms of the characteristic of motion of the source that it moves at the constant velocity v on a rectilinear trajectory distant by d from the static observer. Moreover, it can be assumed arbitrarily that the source passes the observer at the time $T = 0$. (Hence, the negative time half-axis corresponds to the source approaching the observer, the positive to the source moving away from the observer.)

The instantaneous values of the frequency $f(t)$ of the signal and the corresponding changes in the intensity level $L(t)$ of the same signal can be represented analytically by the following relations (cf. [5]):

$$f(t) = f_0\left(1 - \frac{v^2 t}{c\sqrt{(vt)^2 + d^2}}\right), \tag{1}$$

$$L(t) = L(d) + 10\log\left\{\frac{d^2}{(vt)^2 + d^2}\left(1 - \frac{4v^2 t}{c\sqrt{(vt)^2 + d^2}}\right)\right\}, \tag{2}$$

where t — the time of the passage of the source with respect to the observer, $L(d)$ — the intensity level of the signal at the moment of the source passing the observer, and c — the propagation velocity of the tonal signal in the medium; with both relations valid under the assumption that $v \ll c$.

Fig. 1 shows, according to relations (1) and (2), the changes in the intensity level $L(t)$ of the signal and the corresponding changes in its frequency $f(t)$ over a 10-second motion of the source in the case when $v = 10$ m/s, $d = 10$ m ($c = 340$ m/s, $L(d) = 90$ dB).

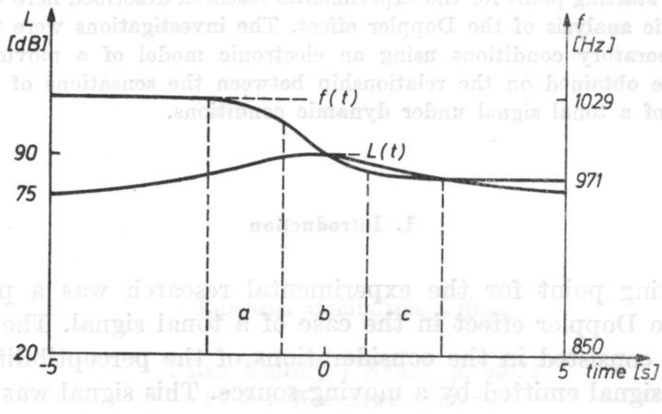

Fig. 1. Changes in the intensity level $L(t)$ of a signal and the corresponding changes in its frequency $f(t)$ over a 10-second motion of the source with respect to the observer ($v = 10$ m/s, $d = 10$ m)

a — the environment of the passage zone caused by the source approaching the observer, b — the passage zone, c — the environment of the passage zone caused by the source moving away from the observer

It follows from Fig. 1 that at both ends of the time interval the frequency changes in the signal are relatively slow compared to the frequency changes in the central part of the time interval under consideration. In the case of the source approaching the observer these changes occur against the background of increasing intensity level, while the source is moving away from the observer — against the background of decreasing intensity level.

Because of the motion characteristic of the source with respect to the observer this two-part area consisting of parts a and c, in which relatively slight frequency changes occur in the tonal signal, was called the environment of the passage zone. (The central part of the interval (*b*) was called the passage zone.) The experimental investigations described in this part of the paper concerned the environment of the passage zone.

2. Methodology of the experimental investigations

In the environment of the passage zone the point of interest was a determination of the dynamic, and at the same time generalized, frequency discrimination thresholds. (Such a definition of the thresholds can be justified by that when the source is moving the signal it emits changes simultaneously its frequency and intensity, and, therefore, the change perceived in the pitch of the signal is a function of two variables. Both physical parameters of the signal are also variable in time, and, therefore, pitch changes are also dynamic (cf. [1]).)

Tests for the psychoacoustic investigations were prepared in the following stages:

1. Tabulation by means of a computer of the instantaneous values of the frequency $f(t)$ and the intensity level $L(t)$ of the signal, according to relations (1) and (2), which occurred at every 10^{-1} s in the case of different velocities v of the motion of the source and different distances d of the motion trajectory from the observer, with the velocity v taking the values 10; 20; 30 m/s, and the distance d being 1; 5; 10 m.

2. Application in the experimental investigations of a purposebuilt electronic model of a moving source (cf. [2]). The results obtained correspond, therefore, only approximately to the real conditions of the Doppler effect perception, since the following factors were not represented in the model of the acoustic field constructed: the spatiality of sound radiation and detection and the damping of the acoustic wave by the medium. The results correspond, therefore, to an explanation of some general phenomena in a simultaneous perception of frequency and intensity changes in simple sounds rather than to detailed investigations of a specific physical effect.

3. Recording on punched tape of the parameters of acoustic signals, i.e. of the instantaneous values of frequency and intensity level, emitted by the source in both parts of the environment of the passage zone. The acoustic signals obtained from the electronic model of the source were turned into tests; the latter, in turn, were recorded on magnetic tape.

4. Presentation of tests by earphones to both ears of a listener.

The component signals of the tests consisted of increasingly longer time intervals when the source approached the observer (A_n) and increasingly shorter ones when the source moved away ($A_{n'}$). In both cases the intervals covered the whole area of the environment of the passage zone (cf. Fig. 2).

The durations of the particular component signals fell in the interval 4-7s, while the number of signals in a test varied between 5 and 17. (The number of signals in a test depended on the width of the environment of the zone passage, and, accordingly, on the distance d of the motion trajectory from the observer.) The order in which the particular components, (A_n or $A_{n'}$), occurred in a test was established by dependent random selection, i.e. each component signal was selected only once for a test.

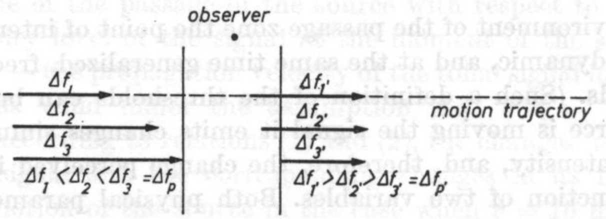

Fig. 2. A diagram for making the relevent test signals in the case of the source approaching the observer $- A_n$, and moving away from the observer $- A_{n'}$; → the signal emitted by the source, Δf_i — the frequency difference occurring in the signal

The pause between the particular component signals was 8s and was devoted to a listener's answer. Each test was begun by the 8-second signal A_0 of constant frequency and amplitude, i.e. a tone of the frequency $f_0 = 1000$ Hz and the intensity level $L(d) = 90$ dB, which corresponded to a signal emitted by the source at the moment of its passing the observer (cf. Fig. 3).

The investigations were performed on four listeners: two women and two men aged 22-30 years (one of them a musician). Before the investigations these listeners were examined audiologically and underwent a series of preliminary training-type investigations.

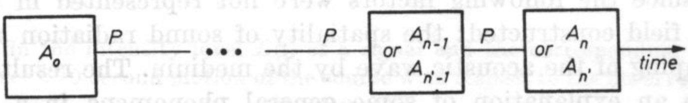

Fig. 3. The diagram of the system of the component signals A_n or $A_{n'}$, used in the experimental investigations; P — the pause

The listener's task was to answer the question as to whether in the course of a given signal (A_n or $A_{n'}$) a change in the frequency of this signal could be perceived, or not. There were two admissible answers: "yes" and "no". Each test was presented 20 times.

3. Analysis of the results

The results of the investigations were represented in the form of psychometric functions which gave the values of the dynamic generalized frequency discrimination thresholds Δf_p, obtained in the case of the source approaching the observer, and $\Delta f_{p'}$, obtained in the case of the source moving away from the observer. Figs. 4 and 5 show examples of the psychometric curve in both cases of the motion of the source with respect to the observer.

The specificity of the present investigations caused the psychometric curves obtained here to be different from the "classical" curves in two respects:

1. Changes in the frequency Δf of the signal are caused by motion of the source; and this fact determines the value of these changes, and, therefore, within successive signals A_n or $A_{n'}$ their frequency does not change by a constant value ($\Delta f \neq \text{const}$).

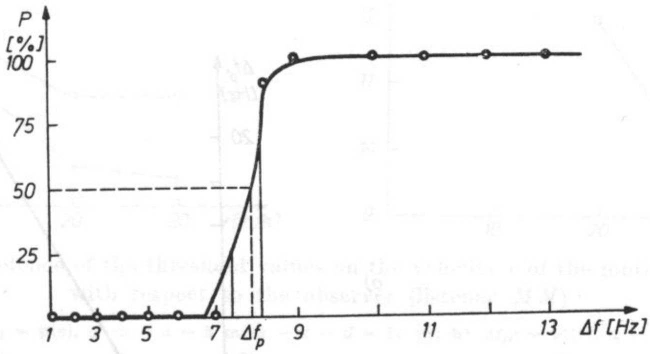

Fig. 4. The results of the experimental investigations in this part of the environment of the passage zone which corresponds to a source approaching the observer ($v = 10$ m/s, $d = 10$ m, $\Delta f_p = 8.30$ Hz, listener MM)

***1* – 1.05, *2* – 1.97, *3* – 2.81, *4* – 3.77, *5* – 4.65, *6* – 5.81, *7* – 7.36, *8* – 9.44, *9* – 10.75, *10* – 13.99, *11* – 15.97, *12* – 18.20, *13* – 20.67**

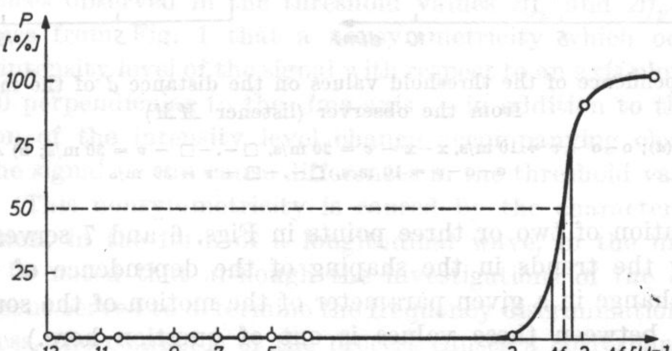

Fig. 5. The results of the experimental investigations in this part of the environment of the passage zone which corresponds to a source moving away from the observer ($v = 10$ m/s, $d = 10$ m, $f_p = 20.02$ Hz, listener MM)

***13* – 1.14, *12* – 2.06, *11* – 3.18, *10* – 3.86, *9* – 5.90, *8* – 6.62, *7* – 7.45, *6* – 8.41, *5* – 9.53, *4* – 10.84, *3* – 18.29, *2* – 20.76, *1* – 23.44**

2. The particular tests presented to listeners consisted of natural Doppler signals from a source in the area of interest, i.e. in both parts of the environment of the passage zone. In none of the signals, therefore, the frequency change Δf was equal to zero. (The signal A_0 emitted at the beginning of each test played the role of a kind of "a reference signal".) As a result of this, the point $\Delta f = 0$ is absent from the abscissa.

Fig. 6 a, b shows the dependence of the threshold values on the distance d of the motion trajectory from the observer. In turn, Fig. 7 a, b illustrates the dependence of the corresponding threshold values on the velocity v of the motion of the source with respect to the observer.

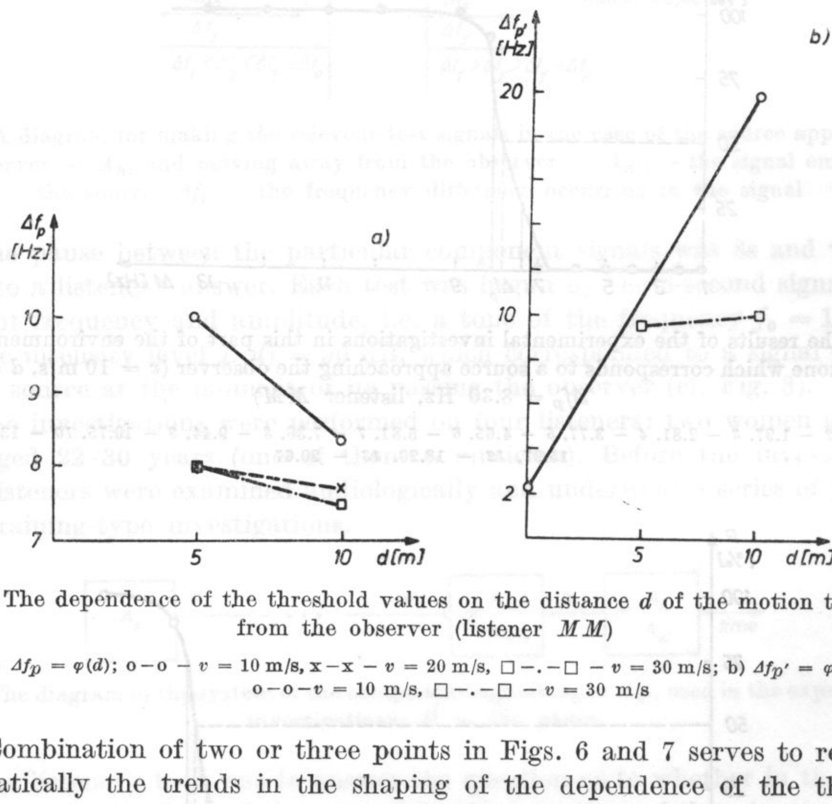

Fig. 6. The dependence of the threshold values on the distance d of the motion trajectory from the observer (listener MM)

a) $\Delta f_p = \varphi(d)$; o–o – $v = 10$ m/s, x–x – $v = 20$ m/s, □–.–□ – $v = 30$ m/s; b) $\Delta f_{p'} = \varphi(d)$; o–o–$v = 10$ m/s, □–.–□ – $v = 30$ m/s

(Combination of two or three points in Figs. 6 and 7 serves to represent schematically the trends in the shaping of the dependence of the threshold values on a change in a given parameter of the motion of the source; and any interpolation between these values is out of question here.)

It was found that the threshold values $\Delta f_{p'}$ are always greater than the corresponding values of Δf_p. This signifies that a change in the frequency of a signal which occurs against the background of decreasing intensity level is less perceptible (in the form of a change in the pitch of this signal) compared to the case when this change occurs against the background of increasing intensity level.

Explanation of the regularities observed should point out the following facts:

1. In signals from a source approaching the observer, i.e. in determination of Δf_p, a difference in the frequency of the signal, which can be perceived as a change in its pitch, occurs in the final time interval of this signal. In a signal from a source moving away from the observer, — i. e. in determination of $\Delta f_{p'}$ —however, this change occurs in the initial interval of the signal.

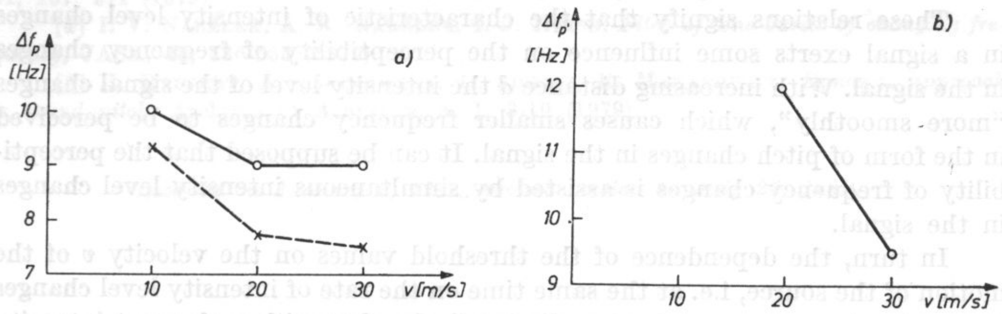

Fig. 7. The dependence of the threshold values on the velocity v of the motion of the source with respect to the observer (listener MM)

a) $\Delta f_p = \psi(v)$, o—o — $d = 5$ m, x — x — $d = 10$ m; b) $\Delta f_{p'} = \psi'(v)$, $d = 5$ m

According to NÁBĚLEK's suggestion [4], the listener estimates the pitch of a tonal pulse of varying frequency on the basis of an excitation model that is formed on the basic membrane at the moment when this pulse is ending. How the frequency of the signal changes in time is, therefore, significant for the process of the perception of the pitch of this signal. As a result, this may lead to differences observed in the threshold values Δf_p and $\Delta f_{p'}$.

2. It follows from Fig. 1 that a nonsymmetricity which occurs in the changes of the intensity level of the signal with respect to an axis plotted through the point $t = 0$ perpendicular to the time axis — in addition to the difference in the direction of the intensity level change accompanying changes in the frequency of the signal — can cause differences in the threshold values Δf_p and $\Delta f_{p'}$ obtained. (This nonsymmetricity is caused by the character of acoustic wave propagation, in the form of a longitudinal wave, in the medium.)

It should be noted that although the investigations of the environment of the passage zone served to determine the frequency discrimination thresholds, but, nevertheless, the character of the process causes a corresponding change in the intensity level of a signal, and also in its duration, to be "ascribed" to each threshold value in the frequency difference Δf_p or $\Delta f_{p'}$ since these values (frequency, intensity level, and duration of the signal) are closely interrelated. An exact analysis of the influence of changes in the intensity level and duration of the signal on threshold values obtained needs further investigations.

It follows from Figs. 6 and 7 that

1. In the case of the threshold values Δf_p:

(a) these values decrease with decreasing distance d, which means that smaller differences in the frequency of a signal are perceived as changes in its pitch;

(b) these values also decrease with increasing velocity v; although the change in the threshold values is different for the velocity change from 10 to 20 m/s than for that from 20 to 30 m/s (for the latter velocity change the threshold values change only very slightly).

These relations signify that the characteristic of intensity level changes in a signal exerts some influence on the perceptibility of frequency changes in the signal. With increasing distance d the intensity level of the signal changes "more smoothly", which causes smaller frequency changes to be perceived in the form of pitch changes in the signal. It can be supposed that the perceptibility of frequency changes is assisted by simultaneous intensity level changes in the signal.

In turn, the dependence of the threshold values on the velocity v of the motion of the source, i.e. at the same time on the rate of intensity level changes in the signal, can be explained preliminarily by that with such great intensity level changes the listener can find it difficult to identify the particular psychoacoustic parameters. He can thus take intensity level changes (which in classical approach correspond to pitch changes) for pitch changes in a signal (cf. under static conditions [1]).

2. In the case of the threshold values $\Delta f_{p'}$:

(a) their dependence on the velocity v of the motion of the source shows the same tendency as in the case of Δf_p;

(b) their dependence on the distance d of the motion trajectory from the observer is, however, contrary to that in the case of the threshold values Δf_p. This partly results from the fact that a full set of these values was not obtained in the case of the determination of the threshold values $\Delta f_{p'}$ (including those for the musician). The perceptibility of frequency changes in a signal under the conditions of a source moving away from the observer was rather difficult for the listeners.

4. Conclusions

On the basis of a psychoacoustic analysis of the Doppler effect data were obtained on relations between the sensations of loudness and pitch under dynamic conditions. It was found that intensity changes can in some cases make it easier, or more difficult in other cases, to perceive frequency changes in a signal. If follows in addition from experimental data that a frequency change in a signal against the background of decreasing intensity level is less perceptible than that against the background of increasing intensity level.

References

[1] A. Czajkowska, *Psychoacoustic analysis of perception and evaluation of simultaneous intensity and frequency variations in tonal signals* (in Polish), doct. diss., Adam Mickiewicz University, Poznań.

[2] U. Jorasz, A. Kamasa, J. Koludo, *Electronic model of a moving source* (in Polish), Archiwum Akustyki, **16**, 4 (1981).

[3] R. Makarewicz, *Intensity of sound field generated by a moving source*, Acustica, **41**, 267, 271 (1979).

[4] I. V. Nábělek, A. K. Nábělek, I. J. Hirsh, *Pitch of tone bursts of changing frequency*, JASA, **48**, 536-553 (1970).

[5] H. Ryffert, A. Czajkowska, U. Jorasz, R. Makarewicz, *Dynamic approach to sound pitch*, Archives of Acoustics, **4**, 1, 3-10 (1979).

Received on January 6, 1981; revised version on July 27, 1981.

ARCHIVES OF ACOUSTICS
7, 1, 13–28 (1982)

TOLERANCE OF INTONATION DEVIATION IN MELODIC INTERVALS IN LISTENERS OF DIFFERENT MUSICAL TRAINING

JANINA FYK

Pedagogical University (65-069 Zielona Góra, Plac Słowiański 25)

The aim of the present experimental paper was to investigate the tolerance of intonation deviations in musical intervals, depending on listeners' musical training. The investigations covered the perception of intonation deviations of chosen melodic intervals in isolation and in melodic context. Tests were edited from music material recorded on magnetic tape and were exposed by a loudspeaker to groups of 8-12 persons. The results obtained confirmed a dominating effect of musical training on the tolerance of intonation deviations in isolated intervals and those in melodic context. It was found out that in a musically trained group the tolerance of intonation deviations in intervals in melodic context was influenced by functional tendency and by the direction of intervals in a musically untrained group.

1. Introduction

In 1924-1925 MORAN and PRATT [14] initiated investigations, aiming at determination of musical interval sizes in a psychoacoustic sense. Establishing the variability range of an interval tuned freely under the conditions of listeners adjusting the frequency of one of tones with respect to a constant reference tone, intonation tolerance zones of the particular intervals were obtained. For intervals of less than octave these zones were 13-22 ct.

In more recent papers a similar direction of investigation was followed by WARD [26], DROBNER [4], TARNOCZY and SZENDE [25], SUNDBERG and LINDQVIST [24], OSSOLIŃSKA-SIEŃCZEWSKA [17], LIPPUS, REMMEL and ROSS [12], and RAKOWSKI [20]. These research workers confirmed that interval estimation is based on a sensation of its size, which does not always coincide with frequency ratio estimation. All of the above mentioned investigations were performed on isolated intervals. The experiments consisted in free tuning of an interval or estimation of its magnitude.

Apart from this direction, intonation was investigated on the basis of instrumental and vocal recordings of parts of pieces of music. In his investigation of melodic intervals on the basis of a gramophone recording of Violin Etude No. 2 by Kreutzer, GREENE [7] found out that the dominating intonation pattern is one close to the Pythagorean system. The same conclusion was also reached by NICKERSON [15]. It was GARBUZOV's investigation [6] of intonation that proved that the key in which vocal and instrumental pieces in untempered system are performed is a twelve-zone system, and the pitch of a musical sound, symbolized by a discrete value of frequency, is psychologically a pitch zone of some width. The zonal theory of GARBUZOV was further developed in investigations of the interval intonation in melodic structures carried out by RAGS [19] and SAKHALTUEVA [21, 22] and works of BURNS [1], BURNS and WARD [3], and in RAKOWSKI [20], devoted to a categorical perception of intervals. RAGS and SAKHALTUEVA tried to grasp and explain the regularity of intonation deviations occurring in the performance of a melody on instruments of untempered system. They have found that clear intonation is a variable quantity closely related to a tonal design of a piece and to the creative purposes of the artist. Being one of elements of musical expression, intonation is specifically related to a whole series of elements of a piece of music: the design of melody, harmony and rhythm, dynamics and elements of musical form.

The results of these investigations have proved that a musical context is a dominating cause of intonation deviations. The effect of musical context on the perception of intervals was also stressed by other research workers: FRANCÈS [5], SHACKFORD [23], LEIPP [11], PATTERSON [18], HARAJDA and FYK [8], WRONKOWSKA [27].

A common feature of the previous investigations in the field of interval perception was the participation in these investigations of listener groups uniform in terms of musical training and most frequently highly trained. The conclusions drawn from these investigations applied, therefore, only to this narrow listener community. On the basis of the previous investigations [16, 10, 2, 13, 3, 20], which stressed the role of musical training and showed that the perception of intonation deviations in intervals was conditioned by previous practice, qualitative differences in the perception of interval intonation deviations of the same size could be expected in listeners representative of different musical training.

Detection and analysis of these differences was the aim of the present paper, and since there are only a few papers on a joint investigation of the perception of intervals in isolation and in melodic structures [8, 9, 27], the author decided to make comparisons also in this respect. However, with its present limited investigation material, this paper does not aim to explain fully the reasons for these differences and the laws which governed them. It presents only an initial stage of this investigation.

The investigations were performed for chosen melodic intervals in isolation and in melodic context. The following isolated intervals were used: prime (1), minor second intoned upwards ($2m\uparrow$), major second intoned downwards ($2w\downarrow$) and minor third intoned downwards ($3m\downarrow$). The first three intervals and also a major seventh ($7w$) were investigated in melodic context. 1,$2m$, $2w$ and $3m$ were selected, since these intervals most frequently occur in melodies and, to a large extent, are melody components, which was confirmed by ORTMANN's investigations [16]. $7w$ was selected as an interval in strong contrast to features of the intervals mentioned above.

Since intervals in a melody are elements of some superior whole, it is important to select a melodic context which favours the individualization of intervals, i.e. which permits a diversity of intonation deviations. Melodies composed for this purpose included intervals built from degrees of low intonation stability (IInd and VIIth degrees of the scale).

2. Criteria for selection of the group

The experiment was performed on three first-year students of pedagogy departments of Pedagogical University, Zielona Góra. Selection of students to the particular groups was based on their musical training. Additionally, the following criteria were applied to all persons participating in the experiment: otolaryngologically normal hearing and good intonation accuracy. Hearing was examined audiometrically twice and the curves of the audibility threshold were determined separately for each ear. Only those persons in whom the hearing loss did not exceed the medical norm participated in these experimental investigations. Examination of intonation accuracy permitted persons having difficulties with clear intonation (13 persons) to be eliminated. Most of these were found to have a high pitch discrimination threshold (of about 10 Hz for a reference frequency of 440 Hz). Eventually, 20 students of the Pre-School Pedagogy Department without any musical training were assigned to the first group. The second group of 30 persons was made up of the Initial Education Department who had learned to play an instrument for two to four years (except one, all the listeners had graduated from secondary level schools for kindegarten personnel). The third group of 20 persons included students of the Musical Education Department with seven years on average of musical training. The listeners in the above groups took part in listening tests of the tolerance of intonation deviations in intervals in isolation and of those in melodic context.

3. Composition of tests

The tests were developed for sinusoidal tones (the test of the tolerance of intonation deviations in isolated intervals) and for piano sounds (the test of the tolerance of intonation deviations in intervals in melodic context). Detailed data on the programming of a test of sinusoidal tones were given in the description of an earlier experiment devoted to the investigation of the perceptibility of mistuned melodic intervals in secondary school students [9]. The test made up of piano sounds was also recorded under analogous conditions and using the same measurement apparatus as in the experiment mentioned above.

3.1. *The test of the tolerance of intonation deviations in isolated intervals consisted of 4 series.* The first series concerned the tolerance of intonation deviations of the prime (1); the second series — the minor second intoned upwards (*2m*↑), the third — the major second intoned downwards (*2w*↓), and the fourth series — the minor third intoned downwards (*3m*↓). Each series included 12 pairs of intervals, of which, in 10 pairs, the first interval was the standard one, while the second interval called the variable interval showed intonation deviation in the second sound of the interval; in the other two pairs only intervals without intonation deviations (standard intervals) occurred. The standard interval of a given interval was an intonation variant of the interval which corresponded to the size of the interval in a well-tempered system. The sizes of intonation deviation were 10, 15, 25, 50 and 75 ct, upwards and downwards. In order to make possible the comparison of the tolerances of intonation deviations in intervals in isolation and in melodic context, in both cases the same direction and pitch register of an interval were maintained, with, however, a basic difference: the second interval in a pair of isolated intervals was not transposed, while the second melody of a test pair which contained a variable interval was transposed. Test tasks were presented in an almost stochastic order. The listeners' task was to estimate whether there was a perceptible difference between the intonation of the second sound in the standard interval and that of the variable interval.

3.2. *The test of the tolerance of intonation deviations in intervals in melodic context consisted of 7 series comprising test melodies with the following intervals included*: series I — the prime which was a repetition of the lower keynote (1 I → I degree), series II — the minor second in direction from VII to VIII degree (*2m* VII → VIII), series III — the minor second in direction from VIII to VII degree (*2m* VIII → VII), series IV — the major second in direction from I to II degree (*2w* I → II), series V — the major second in direction from II to I degree (*2w* II → I), series VI — the major seventh in direction from VII to I degree (*7w* I → VII), series VII — the major seventh in direction from VII to I degree (*7w* VII → I). Each series consisted of 20 pairs of a two-bar melody in major key. The first melody was the standard, while the other was a transposition of the former by an interval of *2w* upwards. The second melody was transposed with respect to the standard so as to avoid the listeners comparing the final sounds of both melodies in terms of pitch instead of interval size. In the transposed melody every second case featured intonation deviation in the last sound, whose size was, respectively, 5, 10, 15, 25 and 50 ct upwards and downwards. A pair of melodies composed of the standard and the transposed melody constituted one test task. An example of the test task is shown in Fig. 1.

The intervals *2m*, *2w* and *7w* always occurred in two melodic contexts: in the first one the melody defined the harmonic content finished with a cadence,

Fig. 1. An example of a test task in series I of the test of the tolerance of intonation deviations in intervals in melodic context

melody *s* – the standard melody, melody *t* – the transposed melody, p^1 – the pause between a pair of melodies, p^2 – the answer time

Fig. 2. Music material of successive series of the test of the tolerance of intonation deviations in intervals in melodic context

melody *s* – the standard melody, melody *t* – the transposed melody, I, II, VII, VIII – degrees of a major key. In brackets variable intervals and in the second one with a semi-cadence. Application of intervals in different melodic contexts served to show the influence of the interval harmonic tensions in a melody, which resulted from the harmonic tendency, on the tendency and tolerance of intonation deviations. Music material of the successive test series is shown in Fig. 2.

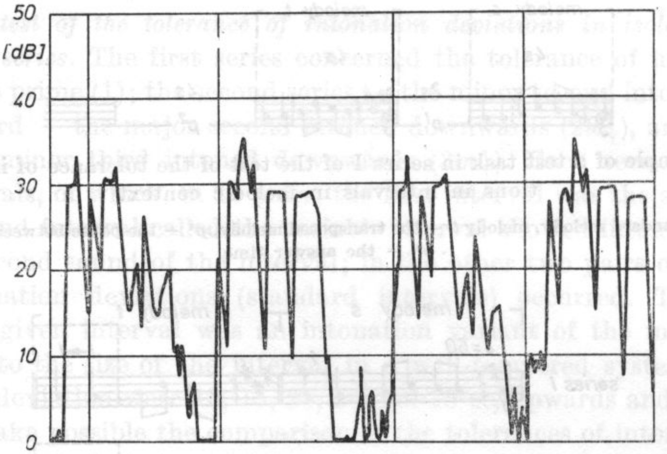

Fig. 3. The time behaviour of amplitude in two successive tasks in series I of the test of the tolerance of intonation deviations in intervals in melodic context

Fig. 3 shows amplitude changes in the course of two successive test tasks performed on the piano. The test melodies ended with a prime interval (1 I → I) without intonation deviation. They were recorded by a PSG-101 recorder. It can be seen that the amplitude variability range of the interval investigated did not exceed 2 dB.

After listening to each pair of melodies the task was to estimate whether there is a perceptible difference between the intonation of the final sound in the standard and that of the transposed melody. The tests were presented from a tape recorder by one loudspeaker column facing the listeners. The sound reproduction level of the test of sinusoidal tones varied from 40 to 60 phons and that of piano sounds from 60 to 70 phons. The listenings of the tests were performed in groups of 10 to 12 persons.

4. Analysis and discussion of the results

The results of the investigation of the tolerance of intonation deviations in intervals in isolation and in melodic context were represented by psychometric curves. Fig. 4 shows the psychometric curves of three listener groups for the isolated intervals 1 and $2m\uparrow$, while Fig. 5 shows these also for the isolated intervals $2w\downarrow$ and $3m\downarrow$. The psychometric curves of three listener groups for

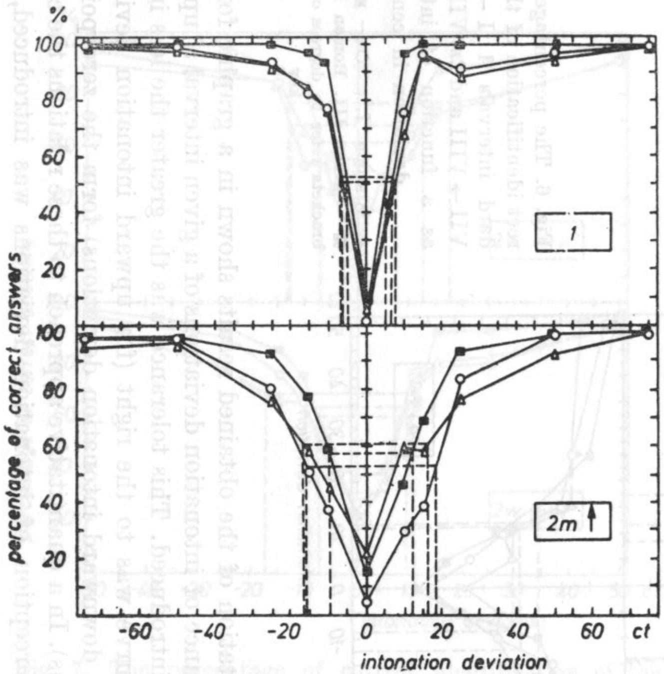

Fig. 4. The percentage of correct identification of the standard intervals of the prime (1) and the minor second intoned upwards (2m↑) as a function of intonation deviation in cents

△ – group I, ○ – group II, ■ – group III

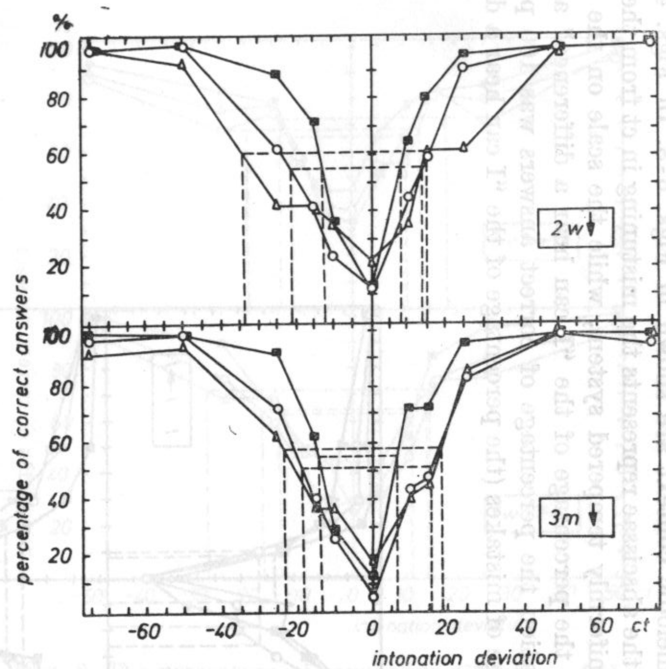

Fig. 5. The percentage of correct identification of the standard intervals of the major second intoned downwards (2w↓) and of the minor third intoned downwards (3m↓) as a function of intonation deviation in cents

△ – group I, ○ – group II, ■ – group III seven intervals in melodic context are shown in Figs. 6-8. In Figs. 4-8 the scale on the axis of the abscissae represents the mistuning in ct from the values determined by a uniformly tempered system, while the scale on the axis of the ordinates gives the percentage of the "I can hear a difference" answers. For a lack of deviation the percentage of correct answers was 100 per cent minus the percentage of mistakes (the percentage of the "I can hear a difference" answers).

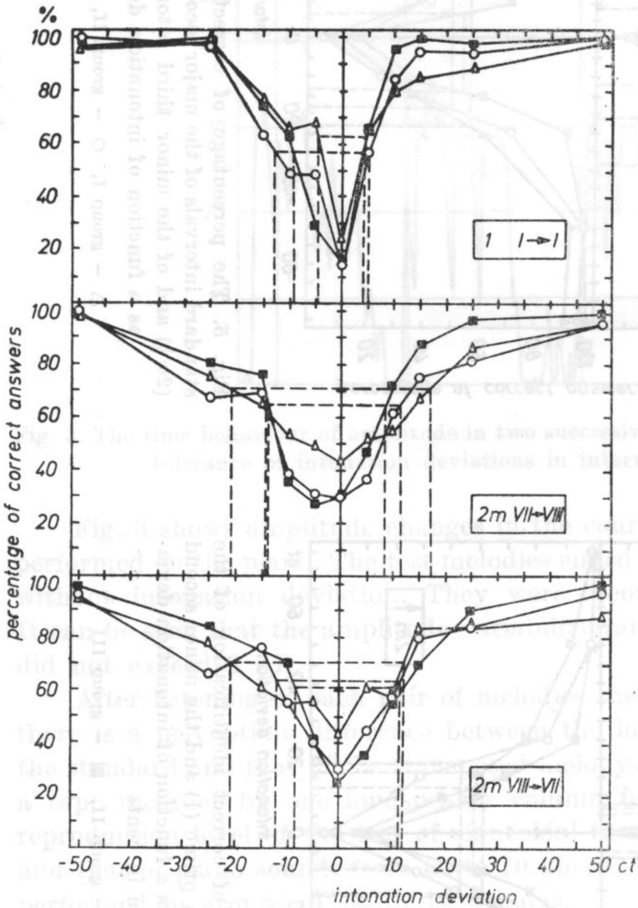

Fig. 6. The percentage of correct identification of the standard intervals 1 I → I, 2*m* VII → VIII and 2*m* VIII → VII as a function of intonation deviation in cents

△ – group I, ○ – group II, ■ – group III. Roman letters in brackets refer to degrees of a major key

In the interpretation of the obtained results shown in a graphic form the concept of the tolerance of intonation deviations of a given interval a) upwards, b) downwards was introduced. This tolerance was the greater the less inclined the psychometric curve was to the right (for upward intonation deviations) and to the left (for downward intonation deviations) form the zero point (no intonation deviations). In a quantitative approach to these relations the concept of the threshold perception of intonation deviations was introduced, being

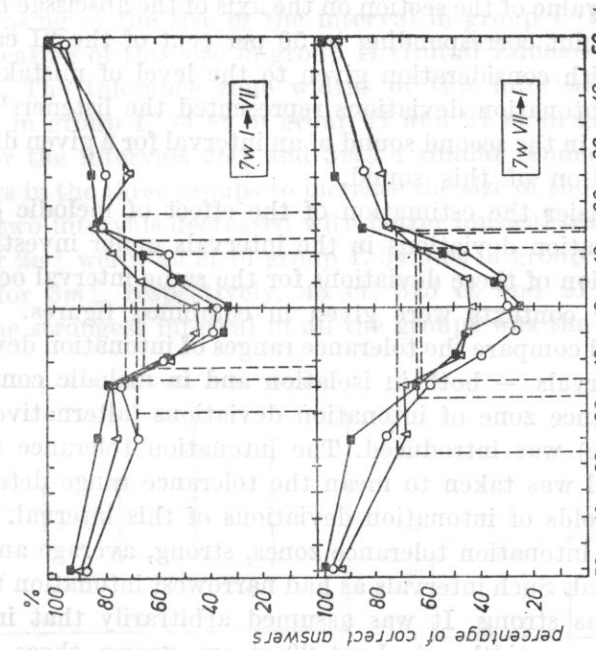

Fig. 8. The percentage of correct identification of the standard intervals 7w I → VII and 7w VII → I as a function of intonation deviation in cents

Δ – group I, ○ – group II, ■ – group III. Roman letters in brackets refer to degrees of a major key

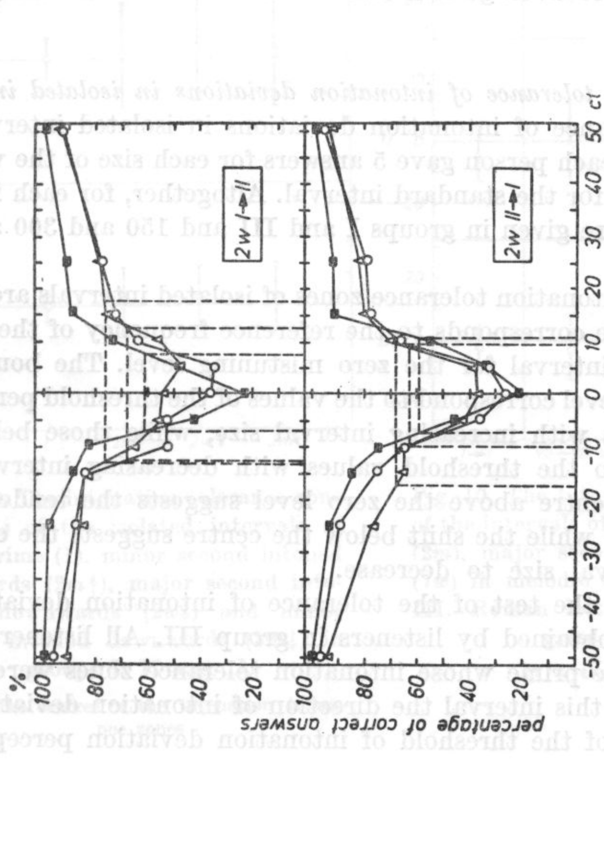

Fig. 7. The percentage of correct identification of the standard intervals 2w I → II and 2w II → I as a function of intonation deviation in cents

Δ – group I, ○ – group II, ■ – group III. Roman letters in brackets refer to degrees of a major key defined arbitrarily as the value of the section on the axis of the abscissae between the zero point and the point corresponding to 50 per cent of the "I can hear a difference" answers, with consideration given to the level of mistakes. The threshold perception of intonation deviations represented the listeners' ability of detecting pitch changes in the second sound of an interval for a given direction of the intonation deviation of this sound.

In order to make easier the estimation of the effect of melodic context on the tolerance of intonation deviations in the intervals under investigation, the results of the perception of these deviations for the same interval occurring in two different melodic contexts were given in combined figures.

In order to define and compare the tolerance ranges of intonation deviations in standard melodic intervals — both in isolation and in melodic context — the concept of the tolerance zone of intonation deviations (alternatively, the intonation tolerance zone) was introduced. The intonation tolerance zone of a given standard interval was taken to mean the tolerance range determined by the perception thresholds of intonation deviations of this interval. On the basis of the width of the intonation tolerance zones, strong, average and weak intervals were distinguished. Such intervals as had narrowest intonation tolerance zones were assumed as strong. It was assumed arbitrarily that intervals of intonation tolerance zone widths of about 20 ct are strong, those of zone widths of about 25 ct are average and those of zone widths exceeding 30 ct are weak.

4.1. *Analysis of the tolerance of intonation deviations in isolated intervals.* In the test of the tolerance of intonation deviations in isolated intervals for the particular intervals each person gave 5 answers for each size of the variable interval and 10 answers for the standard interval. Altogether, for each interval 100 and 200 answers were given in groups I and III and 150 and 300 answers in group II.

The widths of the intonation tolerance zones of isolated intervals are shown in Fig. 9. The zero value corresponds to the reference frequency of the second sound of the standard interval for the zero mistuning level. The boundaries of zones above the zero level correspond to the values of the threshold perception of intonation deviations with increasing interval size, while those below the zero level correspond to the threshold values with decreasing interval size. The shift of the zone centre above the zero level suggests the tendency for interval size to increase, while the shift below the centre suggests the opposite tendency, i.e. for interval size to decrease.

The best results of the test of the tolerance of intonation deviations in isolated intervals were obtained by listeners in group III. All listeners found it easiest to perceive the prime whose intonation tolerance zones were in the limits 14.5-10.5 ct. For this interval the direction of intonation deviation had no effect on the value of the threshold of intonation deviation perception.

Two opposite tendencies were observed to occur in the interval $2m\uparrow$: a decreasing of the size of the interval in group I (Pre-School Pedagogy) and an increasing of this size in group II (Initial Education) and III (Musical Education). The tolerance zone widths of this interval were different and were 28.5 ct in group I, 34 ct in group II and 21 ct in group III.

For the intervals $2w\downarrow$ and $3m\downarrow$ a similar tendency could be observed for listeners in the three groups to increase the size of the intervals. The zone widths of the two intervals decreased with better musical training of persons examined and for $2w\downarrow$ were: 49 ct in group I, 34.5 ct in group II and 21 ct in group III, while for $3m\downarrow$, respectively, 43 ct, 345 ct and 21 ct.

The strongest interval in all the groups was the prime the narrowest into-

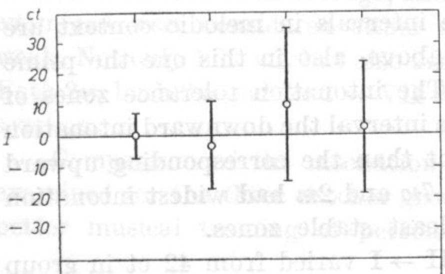

Fig. 9. The intonation tolerance zone widths of the isolated intervals of the prime (1), minor second intoned upwards ($2m\uparrow$), major second intoned downwards ($2w\downarrow$) and minor third intoned downwards ($3m\downarrow$) in groups I, II and III

○ – the centres of the intonation tolerance zones

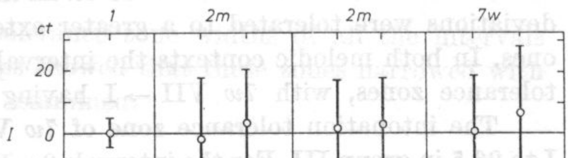

Fig. 10. The intonation tolerance zone widths of the intervals of the prime (1), minor second ($2m$), major second ($2w$) and major seventh ($7w$) in melodic context in groups I, II and III. Roman letters in brackets refer to degrees of a major key

○ – the centres of the zones

nation tolerance zone. In group III the strong intervals were all the other intervals, i.e. $2m\uparrow$, $2w\downarrow$ and $3m\downarrow$, while the same intervals were weak in groups I and II.

4.2. *Analysis of the tolerance of intonation deviations in intervals in melodic context.* In the test of the tolerance of intonation deviations in intervals in melodic context, for the particular intervals each person gave 5 answers for each of 10 intonation deviations in an interval and 50 answers for a standard interval. Thus, a total of 100 answers were obtained in groups I and III for each of the ten intonation deviations in an interval examined and that of 1000 answers for a standard interval. Analogously, 150 and 1500 answers, respectively, were obtained in group II.

The intonation tolerance widths of the intervals in melodic context are shown in Fig. 10. As in the test described above, also in this one the prime (1 I → I) was the most easily perceptible. The intonation tolerance zones of this interval were in the limits 9 - 18 ct. In this interval the downward intonation deviations were tolerated to a greater extent than the corresponding upward ones. In both melodic contexts the intervals *7w* and *2m* had widest intonation tolerance zones, with *7w* VII → I having least stable zones.

The intonation tolerance zone of *7w* VII → I varied from 42 ct in group I to 26.5 in group III. For the intervals *2m* VII → VIII and *7w* VII → I common trends in perception occurred in three listener groups: a decrease in the size of *2m* and an increase in the size of *7m*. These trends agreed with the results obtained by GARBUZOV [6], SAKHALTUEVA [21, 22] and SHACKFORD [23]. In addition the low stability of the intonation tolerance widths of the intervals *2m* VIII → VII and *7w* I → VII, which occurred in the present experiment, where the second sound is the VIIth degree of the key, confirms the SAKHALTUEVA's conclusion [21, 22] as to the considerable width of the intonation deviation zones of the VIIth degree of the key. For the interval *7w* I → VII "average thresholds" occurred in two listener groups. The values of these thresholds were obtained by averaging two threshold values for listeners in these two groups, i.e. 8 ct and 28 ct in group I and 14 ct and 27 ct in group II. The "average thresholds" suggested difficulties in perceiving *7w* I → VII caused by a weak memory trace of this interval, which thus prevents its exact identification. These difficulties were also pointed out by RAKOWSKI's investigations [20] on the differences between the manners of identifying strong and weak intervals (RAKOWSKI [20] distinguished between strong and weak intervals on the basis of the "interval strength" which he identified with the strength of the memory trace established in the long-term memory of listeners).

Different widths of intonation tolerance zones of the same interval when it occured in two different melodic contacts suggested that the context prevented the treatment of the size of a given interval only from one point of view, which agreed with the results of other authors [5, 9, 21, 22, 23, 27]. Considerable differences in the widths of intonation tolerance zones which occurred between different listener groups could be explained by the variously sensed activity of the second sound of the interval in a given melodic context. E.g. while in group I 7*w* I → VII was a weak interval, it was strong in group III. It seems that the increasing stability of the intonation tolerance zones of the intervals examined resulted from a stronger memory trace established in the listeners' memory, which was directly related with the intensity of musical training.

On the basis of the intonation tolerance zone widths 1 I → I was taken in group I as strongest, 2*w* I → II and 2*w* II → I as average, and both 7*w* and both 2*m* as weak. In group II 1 I → I was also strongest, 2*w* II → I strong, both 2*m* and 2*w* I → II average, and both 7*w* weak. In group III all the intervals examined were considered either strong or average, none being regarded as weak. Not only 1 I → I, but also 2*w* I → II were strongest in this listener group. Both 2*w*, both 2*m* and 7*w* I → VII were strong; only 7*w* VII → I was considered average.

Comparison of the intonation tolerance zone widths of all the intervals examined for the three listener groups showed that these zones narrowed with better musical training of persons examined.

5. Conclusions

On the basis of the data on the tolerance of intonation deviations in melodic intervals in isolation and in melodic context the following conclusions could be drawn:

1. Both in intervals in isolation and those in melodic context a dominating influence on the tolerance of intonation deviations from a standard interval was exerted by the musical training level of persons examined; the higher the musical training level was the lower was the tolerance of intonation deviations. These relations were represented by different intonation tolerance zone widths which decreased for listeners in groups II and III (Figs. 9 and 10).

2. General perception trends occurred for the isolated intervals 2*w*↓ and 3*m*↓, which consisted in the greater tolerance of intonation deviations in agreement with the direction of the motion of the interval. This is confirmed by the asymmetrical behaviour of the psychometrical curves of these intervals for all the listener groups (Fig. 5).

3. The tolerance of pitch hearing of intonation deviations of isolated intervals and that in melodic context were not the same. This could be seen in the greater tolerance of intonation deviations of the isolated prime (Figs. 4 and 9) and of the major second (Figs. 7 and 10), and in the lower tolerance of deviations in these intervals when in melodic context (1 I → I, Figs. 6 and 10, and 2*w* II → I, Figs. 7 and 10). For all the listener groups the prime was the stron-

gest interval both in isolation and in melodic context. Different widths of the intonation tolerance zones of intervals examined in melodic context permitted the distinction into strong intervals (both $2m$ and $7w$ I → VII in listener group III and $2w$ II → I in listener group I), average intervals (both $2m$ and $2w$ I → II in listener group $7w$ and both $2m$ in listener group I) and weak intervals (both $7w$ and both $2w$ in listener group I). Of intervals in isolation, while the strong intervals in group III were $2m\uparrow$, $2w\downarrow$ and $3m\downarrow$, the same intervals were weak in groups I and II.

4. In a musically trained group the tolerance of intonation deviations in intervals in melodic context was influenced by functional tendency, which led to a lowering of the Ist degree in the interval of the prime (1 I → I, Fig. 6) and a raise of the VIIth degree in the interval of the minor second ($2m$ VIII → VII, Fig. 6), with a simultaneous lowering of the latter degree in a musically untrained group. In a musically untrained group the tolerance of intonation deviations is influenced considerably by the direction of interval motion, causing a lowering of the VIIth degree in the interval of the minor second ($2m$ VIII → → VII, Fig. 6), to a lowering of the Ist degree in the interval of the major second ($2w$ II → I, Fig. 7) and in that of the major seventh ($7w$ VII → I, Fig. 8), and to a raise of the IInd degree in the interval of the major second ($2w$ I → II, Fig. 7).

5. Comparison of the intonation tolerance zone widths of intervals in melodic context showed that the melodic context favoured differentiation in interval strength.

The quantitative and qualitative differences in perceptibility between musically trained and untrained listeners revealed here showed the important role of musical education in development of perceiving abilities.

References

[1] E. M. BURNS, *Categorical perception of musical intervals*, 86 Meeting of the Acoustical Society of America, Los Angeles 1973.

[2] E. M. BURNS, *Octave adjustment by non-western musicians*, 88 Meeting of the Acoustical Society of America, St. Louis 1974.

[3] E. M. BURNS, W. D. WARD, *Categorical perception — phenomenon or epiphenomenon : Evidence from experiments in the perception of melodic musical intervals*, JASA, **63**, 456-468 (1978).

[4] M. DROBNER, *New results of investigations of interval hearing zonality* (in Polish), PWSM, Cracow 1967.

[5] R. FRANCÈS, *La perception de la musique*, J. Vrin, Paris 1958.

[6] N. A. GARBUZOV, *Zonnaya priroda zvukovysotnovo swukha*, AN SSSR, Moscow — Leningrad 1948.

[7] P. C. GREENE, *Violin intonation*, JASA, **9**, 43-44 (1937).

[8] H. HARAJDA, J. FYK, *Zonality of melodic intervals in average gifted child* (in Polish), Proc. XXV OSA, Poznań 1978, pp. 131-134.

[9] H. HARAJDA, J. FYK, *The perceptibility of mistuned melodic intervals by school children*, Archives of Acoustics, **6**, 4, 371-384 (1981).

[10] A. J. HOUTSMA, *Discrimination of frequency ratios*, JASA, **44**, 383 (1968).

[11] E. LEIPP, *Acoustique et musique*, Masson et C^le^, Paris 1971.

[12] U. LIPPUS, M. REMMEL, J. ROSS, *Perception of intervals and the theory of virtual pitch*, Izw. AN ESSR, **26**, 281-286 (1977).

[13] P. A. LONG, *Pitch recognition in short melodies*, Abstract of doctoral dissertation, Florida State University, 1975.

[14] H. MORAN, C. C. PRATT, *Variability of judgments on musical intervals*, J. Exp. Psychol., **9**, 492-500 (1926).

[15] J. F. NICKERSON, *Intonation of solo and ensemble performance of the same melody*, JASA, **21**, 595 (1949).

[16] O. ORTMANN, *On the melodic relativity of tones*, Psychological Monograph, **35**, 1-47 (1926).

[17] K. OSSOLIŃSKA-SIEŃCZEWSKA, *Free tuning of isolated intervals* (in Polish), unpublished M. A. thesis, PWSM, Warsaw 1973.

[18] B. PATTERSON, *Violin intonation and musical context: Some suggestions*, unpublished M. A. thesis, Washington University, St. Louis 1978.

[19] J. RAGS, *Intonirovanye melodii v svyazi s nekotorimi yeyo elementami*, Trudy Kafedry Teorii Muzyki Moskovskoy Konservatorii, Muzgiz, Moscow 1960, pp. 338-355.

[20] A. RAKOWSKI, *Categorical perception of pitch in music* (in Polish), PWSM, Warsaw 1978.

[21] O. SAKHALTUEVA, *O nekotorikh zakonomernostyakh intonirovanya v svyazi z formoy, dinamikoy i wadom*, Trudy Kafedry Teorii Muzyki Moskovskoy Konservatorii, Muzgiz, Moscow 1960, pp. 356-378.

[22] O. SAKHALTUEVA, *Intonatsyonnyi analiz ispownenya pervoy chastii kontserta dla skripki s orkestrom Mendelsona, Primanenye akusticzeskikh metodov issledovanya v muzykoznanii*, ed. SKREBKOV, Muzyka, Moscow 1964, pp. 61-78.

[23] C. SHACKFORD, *Some aspects of perception*, Part I and II, J. Mus. Theory, **5**, 161-202 1961; **6**, 66-90 (1962).

[24] J. E. F. SUNDBERG, J. LINDQVIST, *Musical octaves and pitch*, JASA, **54**, 922-929 (1973).

[25] T. TARNOCZY, O. SZENDE, *Experiments on the musical interval sense*, 7th ICA, Budapest 1971, **3**, pp. 685-688.

[26] W. D. WARD, *Subjective musical pitch*, JASA, **26**, 369-380 (1954).

[27] E. WRONKOWSKA, *Intonation of violin intervals* (in Polish), unpublished M. A. thesis, PWSM, Warsaw 1979.

Received on November 2, 1979 ; revised version on May 28, 1981.

ARCHIVES OF ACOUSTICS
7, 1, 29–42 (1982)

PROCESSING OF THE ACOUSTIC WAVE IMAGE

MARIA ANNA DRZEWIECKA, MIECZYSŁAW SZUSTAKOWSKI

WAT (00-908 Warszawa, ul. Lazurowa 224)

This paper presents investigations of a system for processing the image of acoustic wave generated in transparent media. It also gives an analysis of the system and discusses the influence of parameters of spatial filtre apertures and of the acoustic field on the quality of representation of the field intensity distribution.

1. Introduction

Image processing is one of the basic processes of optical information elaboration and involves analysis, transfer and synthesis of an image. A mathematical model of this process is provided by simple and inverse Fourier transforms and by optical multiplication of two functions. In this range, both the analysis of the processing and its physical interpretation have been long known and frequently described [1, 2].

It is different in the case of the processing of a dynamic image, i.e. the image of a progressive or standing acoustic wave (oscillating in time) (Fig. 1b). Interest in the processing of the image of the acoustic wave results mainly from the two respects:

1.1. Visualization of the acoustic field. The processing of the image of acoustic wave allows visualization, analysis and registration of the acoustic field distribution in transparent media (bulk waves) and in opaque media (surface waves). The visual processing and the estimation of the performance of transducers of acoustic waves are highly significant practically, i.e. they permit the analysis and estimation of the performance of piezoelectric and acoustooptic equipment without disturbing the conditions of their work and without damage.

1.2. Optical processing of signals. Most equipment for optical processing of signals uses spectral and correlation signal analysis [3]. The spectral analysis is a component part of the processing system (Fig. 1a), while in the correlation process the image of the signal $S_1(t)$ from the first modulator being processed correlates with the signal $S_2(t)$ in the second acoustooptic modulator (Fig. 1c).

In both cases, what is essential is the problem of exact representation

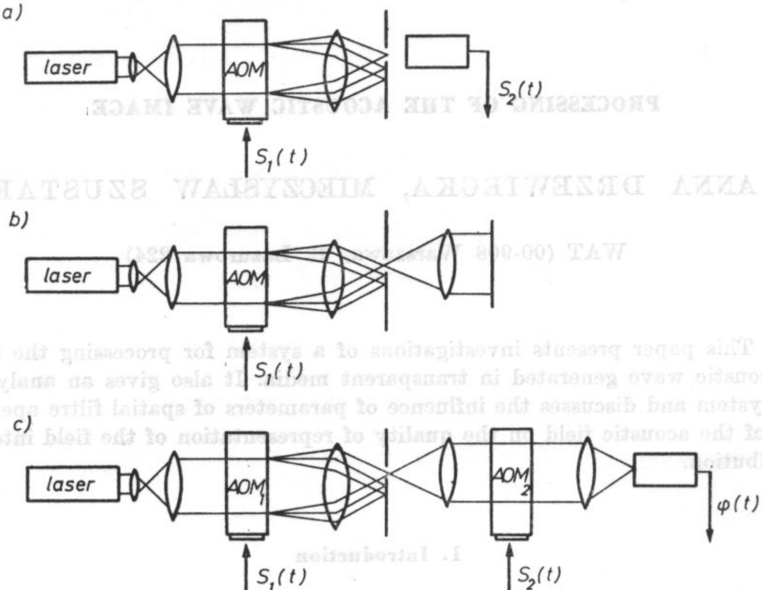

Fig. 1. Image processing in the process of visualization of the acoustic field and acoustooptical processing of signals: a) spectral analysis, b) image processing (visualization of the acoustic field), c) correlation analysis

in the image of both the field intensity distribution and of its shape, particularly in the pulsive performance. In addition, derivation of the signal correlation function [3]

$$\varphi(t) = \int r\left(v_1 t - \frac{M}{n}x\right) S_1(Nt) S_2(v_1 t - nx)\,dx,$$

where $n = v_1/v_2$ is the velocity ratio of acoustic waves in the first and second light modulators, N — the variation degree of the time scale, M — the image magnification; requires the image of the signal $S_1(t)$ to be inverted in time and also the satisfaction of the conditions

$$1 - \frac{M}{n} = -1, \quad N = \frac{M}{n}, \quad \left(v_1 t - \frac{M}{n}x\right) = 1.$$

The inversion of the image, the change of its spatial and time scale, and the representation quality are all implemented in the processing. Therefore, the investigation of the processing of the image of acoustic wave, the determination of the dependence of the parameters of the image on the parameters of the processing system and of the signal of the acoustic wave constitute an essential investigation problem. Investigation of the dependencies mentioned above has also a high practical significance, related to the designing and implementation of both systems for visualization of acoustic fields and acousto-optical processing of signals.

2. Analysis of the system for processing the image of acoustic wave

The processing of the image of acoustic wave was analyzed on the basis of the Raman-Nath diffraction theory. A schematic diagram of the image processing system is shown in Fig. 2.

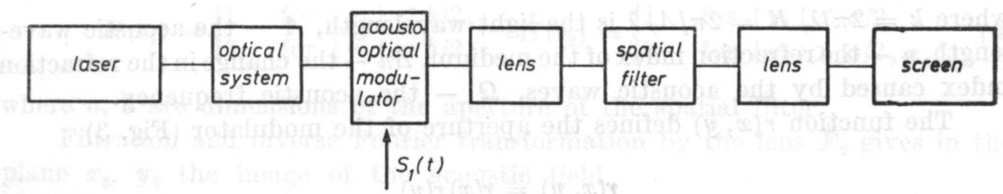

Fig. 2. A schematic diagram of the image processing system

The plane light wave

$$E(x, y, z, t) = E_0\{\exp[i(\omega t - kz)]\} \tag{1}$$

in the plane $z = 0$ falls onto an acoustooptic light modulator with a progressive plane acoustic wave [4]. The propagation direction of the light wave is perpendicular to the direction of the acoustic wave (Fig. 3). In the plane $z = L$

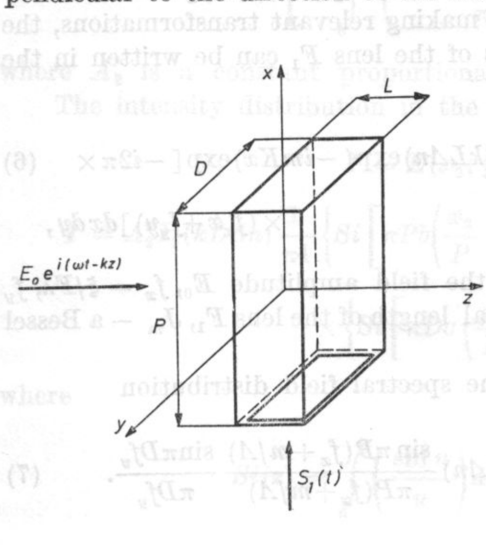

Fig. 3. Acoustooptical light modulator

the light wave has the form

$$E(x, y, L, t) = E(x, y, 0, t)\,T(x, y), \tag{2}$$

where $T(x, y)$ is the transfer function of the modulator,

$$T(x, y) = T_0(x, y)\exp[i\varphi(x, y)]\,r(x, y). \tag{3}$$

Under the assumption that the light wave crosses the acoustic field in a rectilinear manner, the optical nonuniformity related to a change in the refraction index caused by the acoustic wave influences only the phase of the light wave which crosses the acoustic wave stream. Thus, the light propagating in the plane $z = L$ undergoes only phase modulation, and therefore $T_0(x, y) = 1$,

$$\varphi(x, y) = kLn + kL\Delta n\cos(\Omega t - Kx), \tag{4}$$

where $k = 2\pi/\lambda$, $K = 2\pi/\Lambda$, λ is the light wavelength, Λ — the acoustic wavelength, n — the refraction index of the medium, Δn — the change in the refraction index caused by the acoustic waves, Ω — the acoustic frequency.

The function $r(x, y)$ defines the aperture of the modulator (Fig. 3)

$$r(x, y) = r(x)\,r(y),$$

$$r(x) = \begin{cases} 1 & \text{for } |x| \leqslant P/2, \\ 0 & \text{for } |x| > P/2, \end{cases} \qquad r(y) = \begin{cases} 1 & \text{for } |y| \leqslant D/2, \\ 0 & \text{for } |y| > D/2. \end{cases}$$

Thus, the light distribution in the plane $z = L$ can be represented by the relation

$$E(x, y, L, t) = E_0[\exp(i\omega t)]\exp\{ikL[n + \Delta n\cos(\Omega t - Kx)]\}. \tag{5}$$

Using the expansion of the functions of the $\exp(i\cos x)$ type into a series of Bessel functions of the first kind and making relevant transformations, the light amplitude distribution in the focus of the lens F_1 can be written in the form

$$E(\xi, \eta) = A_1 \int_{-P/2}^{P/2}\int_{-D/2}^{D/2}\sum_{m=-\infty}^{\infty}(-i)^m J_m(kL\Delta n)\exp(-imKx)\exp[-i2\pi \times (f_x x + f_y y)]\,dx\,dy, \tag{6}$$

where A_1 is a constant proportional to the field amplitude E_0, $f_x = \xi/F\lambda$, $f_y = \eta/F\lambda$ spatial frequencies, F — the focal length of the lens F_1, J_m — a Bessel function of the first kind of order m.

Integration of equation (6) gives the spectral field distribution

$$E(\xi, \eta) = A_1 PD \sum_{m=-\infty}^{\infty}(-i)^m J_m(kL\Delta n)\frac{\sin\pi P(f_x + m/\Lambda)}{\pi P(f_x + m/\Lambda)}\,\frac{\sin\pi D f_y}{\pi D f_y}. \tag{7}$$

For the sake of the simplicity of notation, the new variable spatial frequencies can be introduced

$$\nu_1 = f_x + m/\Lambda, \quad \nu_2 = f_y. \tag{8}$$

In the domain of spatial frequencies the spectrum undergoes filtration, by multiplication of the spectral function of the acoustic field (7) by the spectral function of the filter $H(\nu_1, \nu_2)$

$$E(\nu_1, \nu_2) = E(\xi, \eta) H(\nu_1, \nu_2),$$

where only the first diffraction order $m = 1$ is filtered.

The filter function has the form

$$H(\nu_1, \nu_2) = H(\nu_1) H(\nu_2),$$

$$H(\nu_1) = \begin{cases} 1 & \text{for } |\nu_1| \leqslant b/2, \\ 0 & \text{for } |\nu_1| > b/2, \end{cases} \quad H(\nu_2) = \begin{cases} 1 & \text{for } |\nu_2| \leqslant a/2, \\ 0 & \text{for } |\nu_2| > a/2, \end{cases} \tag{9}$$

where a, b are dimensions of the aperture of the spatial filter.

Filtration and inverse Fourier transformation by the lens F_2 gives in the plane x_2, y_2 the image of the acoustic field

$$E(x_2, y_2) = \int_{-b/2}^{b/2} \int_{-a/2}^{a/2} (\xi, \eta) H(\nu_1, \nu_2) \exp[i2\pi(\nu_1 x_2 + \nu_2 y_2)] d\nu_1 d\nu_2$$

$$= A_2 J_1(kL\Delta n) \left[iP \int_0^{b/2} \left(\frac{\sin 2\pi\nu_1 (x_2 + P/2)}{\pi\nu_1 P} - \frac{\sin 2\pi\nu_1 (x_2 - P/2)}{\pi\nu_1 P} \right) d\nu_1 \right] \times \tag{10}$$

$$\times \left[iD \int_0^{a/2} \left(\frac{\sin 2\pi\nu_2 (y_2 + D/2)}{\pi\nu_2 D} - \frac{\sin 2\pi\nu_2 (y_2 - D/2)}{\pi\nu_2 D} \right) d\nu_2 \right],$$

where A_2 is a constant proportional to E_0.

The intensity distribution in the acoustic wave image has the form

$$I = E(x_2, y_2) E^*(x_2, y_2),$$

$$I = A_2^2 J_1^2 (kL\Delta n) \frac{1}{\pi 4} \left\{ Si \left[\pi Pb \left(\frac{x_2}{P} + \frac{1}{2} \right) \right] - Si \left[\pi Pb \left(\frac{x_2}{P} - \frac{1}{2} \right) \right] \right\}^2 \times$$

$$\times \left\{ Si \left[\pi Da \left(\frac{y_2}{D} + \frac{1}{2} \right) \right] - Si \left[\pi Da \left(\frac{y_2}{D} - \frac{1}{2} \right) \right] \right\}^2, \tag{11}$$

where

$$Si(z) = \int_0^z \left(\frac{\sin u}{u} \right) du = \frac{1}{2} \int_{-z}^{z} \left(\frac{\sin u}{u} \right) du.$$

The dimensionless product of the field apertures and the *Pb* filter is an analogue of the product $T\Delta f$ in the analysis of time signals. The value of *Pb* or *Da* defines the shape of the field image and affects essentially the quality of representation of the intensity and shape of the input distribution of the acoustic field [5]. Explanation of the effect of the product *Pb* or *Da* on the

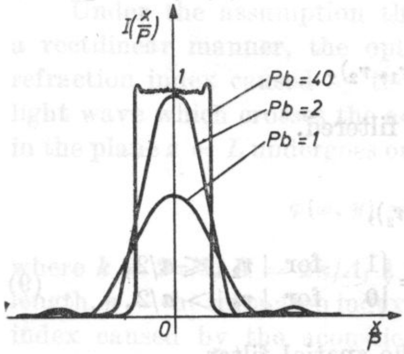

Fig. 4. Light intensity distribution in the image for different values of the product *Pb*

image of the acoustic field is essential for the interpretation of the results of visualization and acoustooptical processing of signals. The present analysis is valid for linear systems, and accordingly the intensity of acoustic fields should be low, thus satisfying the condition of linearity of the system $J_1(kL\Delta n) \approx kL\Delta n/2$. For low intensity of acoustic fields the light intensity distribution in the image is proportional to the acoustic wave intensity. Fig. 4 shows a theoretical field distribution, illustrating the effect of the product *Pb* calculated from expression (11).

3. Experimental investigations

The processing of the acoustic wave image was investigated in the system shown in the diagram (Fig. 5). The acoustic field image was visualized on a TV monitor [6, 7]. The image analysis was performed by the method of electronic image line selection [8]. The system used permitted the field intensity distribution in the acoustic wave image to be registered on the oscilloscope display and recorded on the *XY* plotter.

In the measurements of the acoustic field distribution there occurs a systematic error which results from the processing characteristics of the equipment used and is 6 percent. A more detailed discussion of errors was given in the previous paper [8].

3.1. Processing of the image of a progressive acoustic wave. The investigations of the processing of the acoustic wave image were performed on an acoustooptic modulator with a progressive wave, made of SF6. Transducers of lithium iodate generated a uniform acoustic field of the frequency $f = 50$ MHz. The uniformity of the acoustic field was checked by the method of optical probing in parallel directions.

Fig. 6 shows images of the acoustic wave with the index of the line being selected and theoretical and experimental light intensity distributions in the image

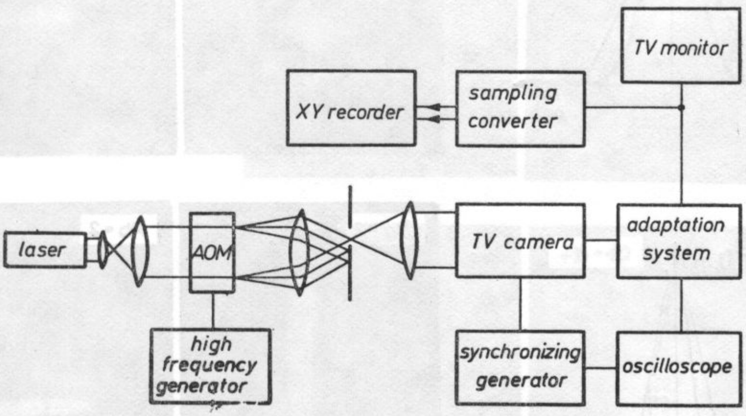

Fig. 5. A block diagram of image processing and analysis

for different values of the aperture product. The values of *Pb* and *Da* were varied by changing the width of the spatial filter; $Pb = 1, 2, 3, 5, 40, 50$ correspond to the widths of the filter aperture 0.01, 0.02, 0.03, 0.05, 0.4, 0.5 mm. For $Da = 1, 2, 3, 5, 40, 50$ the filter widths were, respectively, 0.005, 0.010, 0.015, 0.025, 0.20, 0.25 mm. It follows from the investigations performed that the image of the field is well represented at $Pb > 40$ and $Da > 40$, which corresponds to a filter width comparable with the diameter of the diffracted light stream. At lower values of *Pb* and *Da* the image of the field is not complete and distorted by diffraction effects on the edges of the spatial filter.

The curves of the intensity distribution of the acoustic fields obtained by the method of electronic image analysis are close in shape to the theoretical curves. The differences observed are caused by the additional light scattering on the faults of the modulator crystal (scratches, dust). Nonuniformities of the image background, which are strongest at the edges of the image, are caused by the inertia of the vidicon of the camera and by the presence of the so-called false signals [8].

3.2. Processing of the image of the crossed acoustic fields. In the system described above investigations of the modulator were performed, in which the streams of two acoustic waves of the same frequency and running at the right angle to one another (Fig. 7) were crossed.

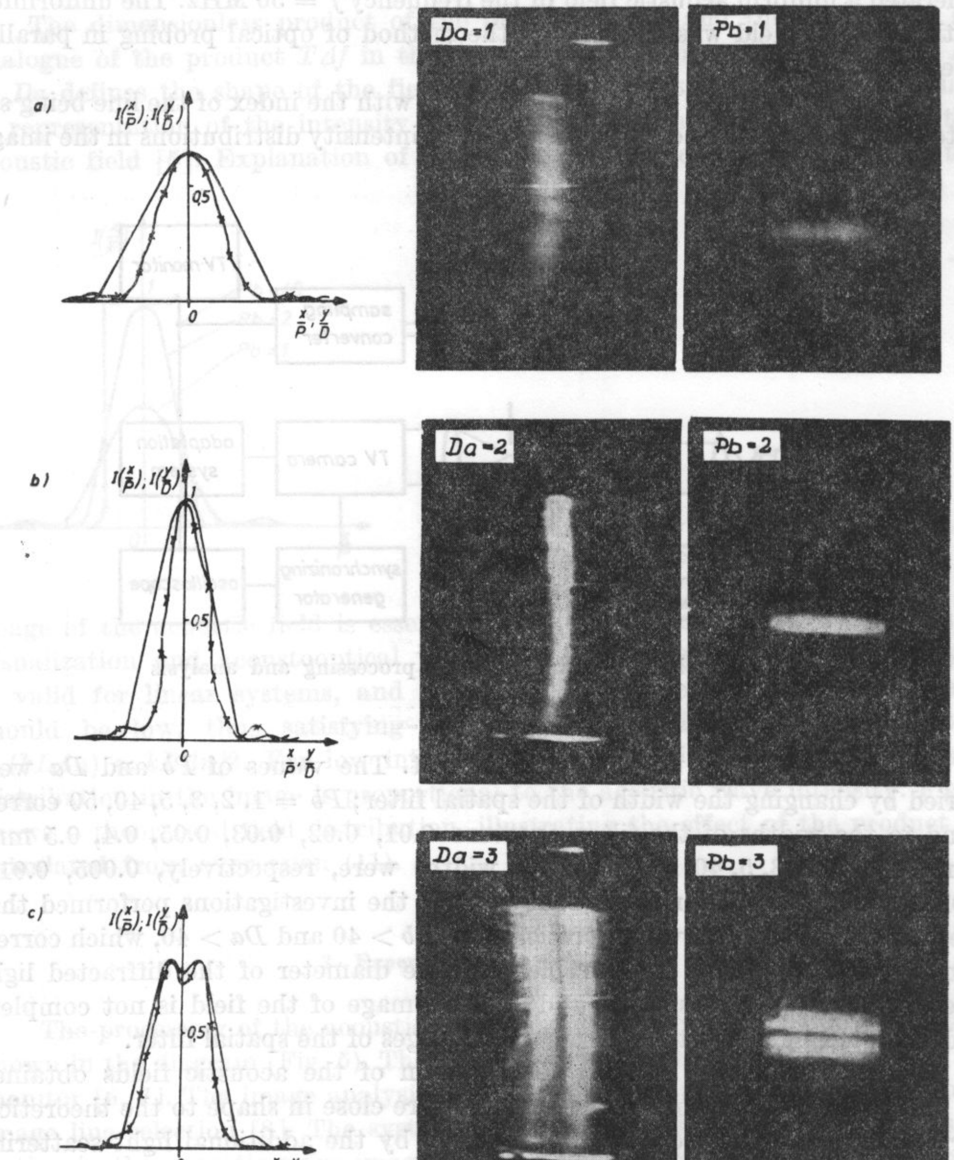

Fig. 6. Acoustic wave images and theoretical (solid lines) and experimental (dash and cross lines) normalized light intensity distributions in the image, illustrating the effect of the aperture product

a) $Pb = 1$, $Da = 1$; *b)* $Pb = 2$, $Da = 2$; *c)* $Pb = 3$, $Da = 3$; *d)* $Pb = 5$, $Da = 5$; *e)* $Pb = 40$, $Da = 40$; *f)* $Pb = 50$, $Da = 50$

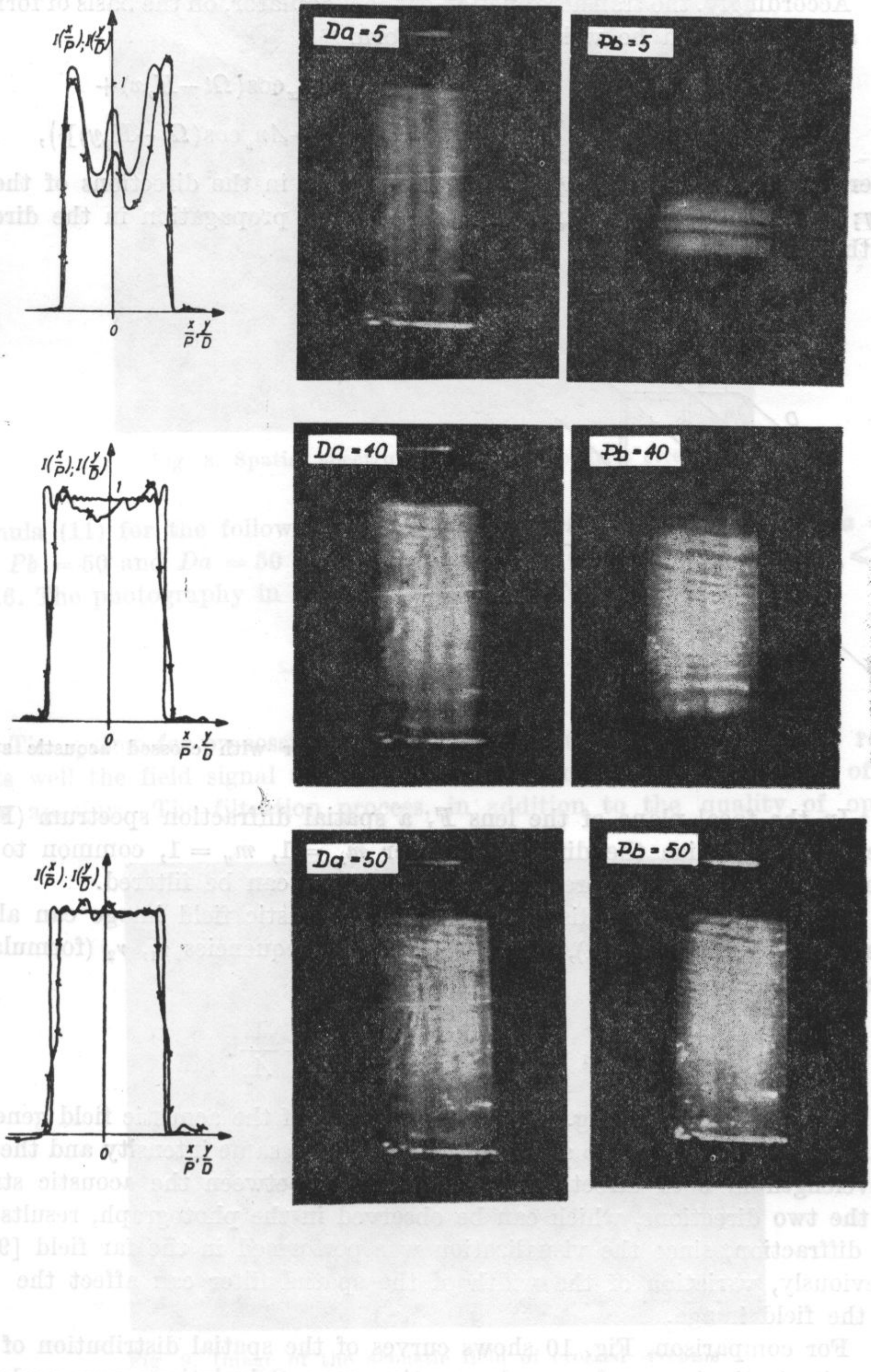
d)
I(x/P); I(y/D)
1
0
x/P; y/D
Da = 5
Pb = 5
e)
I(x/P); I(y/D)
1
x/P; y/D
Da = 40
Pb = 40
f)
I(x/P); I(y/D)
0
x/P; y/D
Da = 50
Pb = 50

Accordingly, the transfer function of the modulator, on the basis of formulae (3) and (4), should be written in the form

$$T(x, y) = T_0(x, y) r(x, y) \exp\big(i\{kLn + kL[\Delta n_x \cos(\Omega t - K_x x) + \Delta n_y \cos(\Omega t - K_y y)]\}\big), \tag{12}$$

where $\Delta n_{x,y}$ are changes in the refraction index in the directions of the axis x, y; and K_x, k_y are constants of acoustic wave propagation in the direction of the axis x and y.

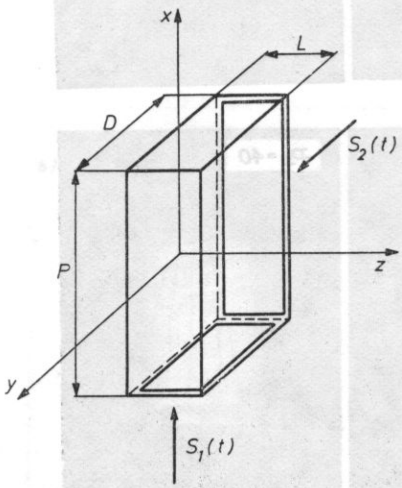

Fig. 7. Modulator with crossed acoustic streams

In the focal plane of the lens F_1 a spatial diffraction spectrum (Fig. 8) occurs, from which the diffraction order $m_x = 1$, $m_y = 1$, common to both acoustic streams and represented by an arrow, can be filtered.

The light intensity distribution in the acoustic field image can also be described by formula (11), where the spatial frequencies ν_1, ν_2 (formula (8)) are inserted in the form

$$\nu_1 = f_x + \frac{1}{\Lambda_x}, \qquad \nu_2 = f_y + \frac{1}{\Lambda_y}.$$

The photography (Fig. 9) shows the image of the acoustic field generated as a result of crossing two acoustic streams of the same intensity and the same wavelength in both directions. The difference between the acoustic streams in the two directions, which can be observed in the photograph, results from its diffraction, since the visualization was performed in the far field [9]. As previously, variation of the width of the spatial filter can affect the shape of the field image.

For comparison, Fig. 10 shows curves of the spatial distribution of light intensity in the image of crossed acoustic waves. Calculations were made from

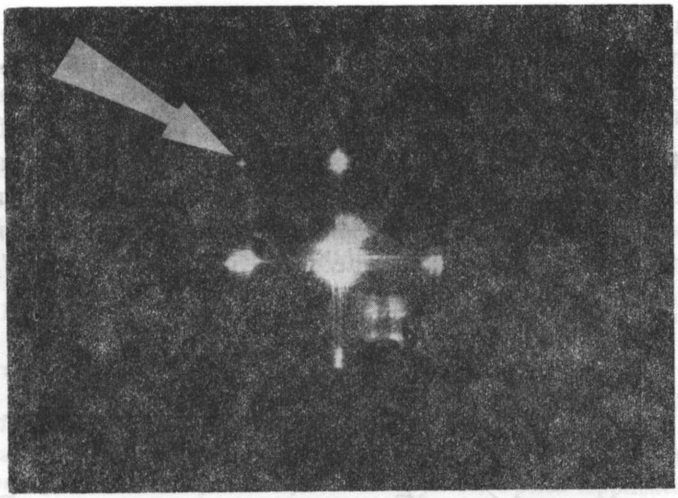

Fig. 8. Spatial spectrum of crossed acoustic streams

formula (11) for the following values of the parameters: $Pb = 40$, $Da = 40$ and $Pb = 50$ and $Da = 50$ and the coordinates $0 \leqslant x/P \leqslant 0.6$ and $0 \leqslant y/D \leqslant 0.6$. The photography in Fig. 9 was taken at $Pb = 30$ and $Da = 30$.

4. Conclusions

The system for processing the acoustic field image constructed here represents well the field signal under the conditions of a correct selection of the filter aperture. The filtration process, in addition to the quality of optical

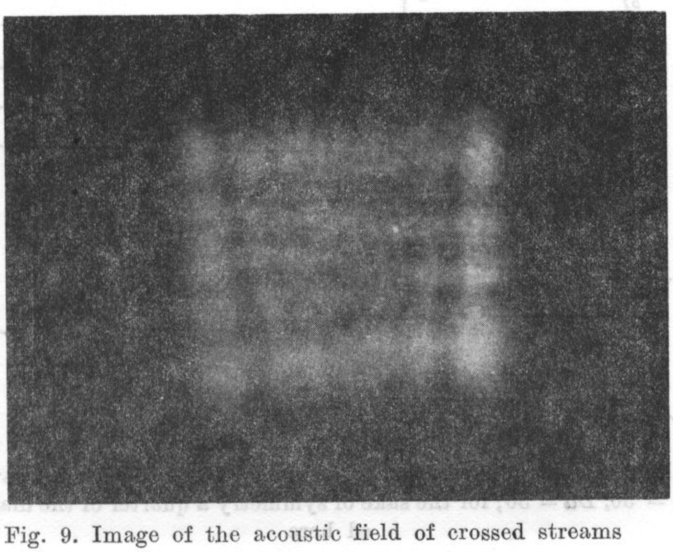

Fig. 9. Image of the acoustic field of crossed streams

elements, has an essential effect on the quality and fidelity of the image. In view to maintaining the linearity of the image processing system, the acoustic fields undergoing optical elaboration should not introduce nonlinear distortions. In employing visualization for the evaluation of the performance of piezoelectric transducers attention should be paid to such selection of a filter that the distortion of the intensity distribution in the image by the filtration process can be avoided. The filtration process is particularly important in the implementation of the correlation function, where the acoustic field of the signal $S_2(t)$ correlates with the optical image of the field of the signal $S_1(t)$.

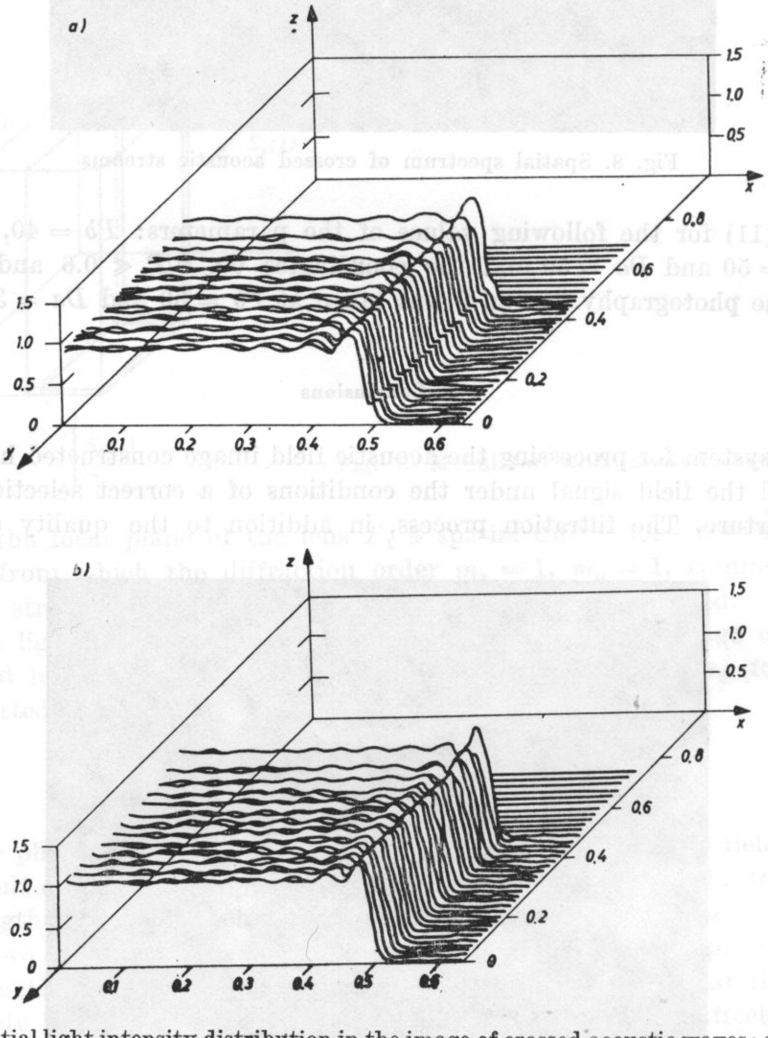

Fig. 10. Spatial light intensity distribution in the image of crossed acoustic waves; a) $Pb = 40$, $Da = 40$; b) $Pb = 50$, $Da = 50$; for the sake of symmetry a quarter of the diagram is presented here

References

[1] A. H. Piekara, *New optics* (in Polish), PWN, Warsaw 1976.

[2] W. T. Cathey, *Optical information processing and holography* (in Polish), PWN, Warsaw 1978.

[3] S. V. Kulakov, *Akustoopticheskie ustroystva spektralnovo i korrelatsyonnovo analiza signalov*, Nauka, Leningrad 1978.

[4] L. B. Lambert, *Wide-band, instantaneous spectrum analyzers employing delay-line light modulators*, Electronics, Research Laboratories, School of Engeneering and Applied Science, Columbia University, 1972.

[5] R. V. Pole, K. S. Penington, *Optical information processing*, Laser Handbook, 1972.

[6] A. Byszewski, A. Drzewiecka, M. Szustakowski, *Parameter measurements and visualization of surface acoustic waves by the optical reflection method* (in Polish), Biuletyn WAT 10/31, 1978.

[7] A. Byszewski, M. A. Drzewiecka, M. Szustakowski, *An application of the methods of coherent optics to investigations of acoustical fields*, Optica Applicata, **X**, I (1979).

[8] M. A. Drzewiecka, M. Szustakowski, K. Turczyński, *Television analysis of the acoustic field image* (in Polish), Biuletyn WAT (in press).

[9] T. Noughi, A. Fukumoto, *Diagnostic study of banded thickness mode transducers by input impedance measurement*, IEEE Trans. on Sonics and Ultrasonics, **SU-20**, 4 (1973).

Received on October 14, 1980 ; revised version on September 3, 1981.

ARCHIVES OF ACOUSTICS
7, 1, 43–59 (1982)

SCATTERING OF ACOUSTIC WAVES ON FREE SURFACE PERTURBATIONS IN AN ELASTIC HALF-SPACE

FRANCISZEK WITOS

Institute of Physics, Silesian Technical University
(44-100 Gliwice, ul. Krzywoustego 2)

This paper considers a semi-infinite, homogeneous and linearly elastic medium with a perturbed free surface. The perturbation is material loss. Using the Green function method, the first Born aproximation is found for the field of displacements dependent harmonically on time and subsequently energy relations for solutions obtained are calculated. The character and magnitude of scattering on the perturbation are thus defined for any mode occurring in a semi-infinite, homogeneous and linearly elastic medium. In addition, the case of perturbation described by periodic functions, which is essential in practice, is analyzed.

Notation

V – the homogeneous isotropic region occupied by the linearly elastic medium,
S – some area belonging to the region V,
(I, J) – a pair defining the character and kind of wave: $I = 0$ the wave falling onto the perturbation, $I = S$ the wave scattered on the perturbation,
J – specifies modes (SH, P, SV, TR, R, L, T),
$U^{(I,J)}(x, t)$ – displacement of the point x caused by a wave defined by (I, J),
$q^{(I,J)}$ – an acoustic Poynting vector for a wave defined by (I, J),
KW_{n-m} – a directional coefficient of power transformation from the wave n into the wave m,
ϱ – the density of the medium,
c, λ, k – the velocity, length and wave vector of a wave,
e_i – the versors of a Cartesian rectangular coordinate system,
x, θ, φ – the spherical coordinates of the tracing vector x.

1. Introduction

Rayleigh waves have recently been the object of large interest. There are many methods of generation of these waves [2]. The most recent method, proposed by HUMPHRYES and ASH [4], uses the transformation of bulk waves on a system of grooves on a free surface. This method can be used for the generation of Rayleigh waves in any elastic medium, and in the hypersonic range it appears to be competitive with respect to the methods used previously. This method, confirmed by experimental works [1, 4, 13] has one theoretical elaboration, which does not exhaust the problem. At the same time there is a number of theoretical papers [9, 10-12], which discuss the transformation in "the other direction", i.e. the transformation of Rayleigh waves on different kinds of free surface perturbations. In these papers, on the basis of field theory and perturbation calculus, expressions were derived for the displacement field of scattered waves in analytical form. These expressions were confirmed by experimental works [7, 8, 13].

The aim of the present investigation is to analyze the transformation properties of such perturbations, determining the behaviour of any wave occurring in a semi-infinite, homogeneous and linearly elastic medium after its passage through the perturbation. In terms of the solution method this paper is a generalization of the considerations of Rayleigh wave scattering given in [6].

2. Waves in a half-space

Let there be

$$V_1 = \{x : x_3 \geqslant 0\}, \quad \text{and let } S_1 = \{x : x_3 = 0\}$$

be a free surface. For this elastodynamic problem the complete system of solutions for displacement fields dependent harmonically on time is formed by the following modes [3]:

(a) a transverse wave polarized parallel to the free surface (the mode SH);

(b) two modes containing a transverse wave polarized perpendicular to the free surface and a longitudinal wave: one mode describes the case of the longitudinal wave falling onto the free surface (the mode designated as P); the other mode describes the case of the transverse wave falling onto the free surface (the mode designated as SV);

(c) a wave containing a longitudinal wave decaying exponentially with increasing x_3 (the mode TR);

(d) a Rayleigh wave (the mode R).

Without decreasing generalization it is only possible to consider the waves of wave vectors of the type

$$\boldsymbol{k}^{(0)} = (k_1^{(0)}, 0, k_3^{(0)}),$$

since this condition can be satisfied by such a coordinate system that the $0X_1$ axis coincides with the projection of the mode propagation direction onto the free surface.

The displacement vectors for the particular modes take then the form:

— for the mode SH

$$u_1^{(0,SH)}(x,t) = u_3^{(0,SH)}(x,t) = 0,$$

$$u_2^{(0,SH)}(x,t) = M\cos k_\beta x_3 \exp[i(k_1^{(0)}x_1 - \omega t)], \tag{2.1}$$

where

$$k_1^{(0)} = -k_T \sin\theta_0 \cos\varphi_0, \quad k_\beta = k_T \cos\theta_0,$$

M is the amplitude;

— for the other modes

$$u_1^{(0,J)}(x,t) = iM[k_1^{(0)0}(F_1\exp(ik_\alpha x_3) + F_2\exp(-ik_\alpha x_3)) - k_\beta \times \times (G_1\exp(ik_\beta x_3) - G_2\exp(-ik_\beta x_3))\exp[i(k_1^{(0)}x_0 - \omega t)],$$

$$u_2^{(0,J)}(x,t) = 0, \tag{2.2}$$

$$u_3^{(0,J)}(x,t) = iM[k_\alpha(F_1\exp(ik_\alpha x_3) - F_2\exp(-ik_\alpha x_3)) + k_1^{(0)}(G_1\exp(ik_\beta x_3) + G_2\exp(-ik_\beta x_3))]\exp[i(k_1^{(0)}x_1 - \omega t)].$$

The quantities F_2, G_2, $-k_\alpha$, $-k_\beta$, $k_1^{(0)}$ and F_1, G_1, k_α, k_β, $k_1^{(0)0}$, which describe the incident and the reflected waves, respectively, occurring in the particular modes, are given by the formulae:

a) for the mode $P\,(J = P)$

$$F_1 = \frac{4k_1^{(0)^2}k_\alpha k_\beta - (k_\beta^2 - k_1^{(0)^2})^2}{4k_1^{(0)^2}k_\alpha k_\beta + (k_\beta^2 - k_1^{(0)^2})^2}\,\frac{1}{k_L}, \quad F_2 = \frac{1}{k_L},$$

$$G_1 = \frac{-4k_1^{(0)}k_\beta(k_\beta^2 - k_1^{(0)^2})}{4k_1^{(0)^2}k_\alpha k_\beta + (k_\beta^2 - k_1^{(0)^2})^2}\,\frac{1}{k_L}, \quad G_2 = 0, \tag{2.3}$$

$$k_1^{(0)} = -k_L \sin\theta_0\cos\varphi_0, \quad k_\alpha = k_L\cos\theta_0, \quad k_\beta = k_T\sqrt{1 - (k_L^2/k_T^2)\sin^2\theta_0};$$

b) for the mode $SV\ (J = SV)$

$$F_1 = \frac{-4k_1^{(0)}k_\beta(k_\beta^2 - k_1^{(0)^2})}{4k_1^{(0)^2}k_\alpha k_\beta + (k_\beta^2 - k_1^{(0)^2})^2}\,\frac{1}{k_T}, \quad F_2 = 0,$$

$$G_1 = \frac{4k_1^{(0)^2}k_\alpha k_\beta - (k_\beta^2 - k_1^{(0)^2})}{4k_1^{(0)^2}k_\alpha k_\beta + (k_\beta^2 - k_1^{(0)^2})^2}\,\frac{1}{k_T}, \quad G_2 = \frac{1}{k_T}, \tag{2.4}$$

$$k_1^{(0)} = -k_T\sin\theta_0\cos\varphi_0, \quad k = k_T\cos\theta_0,$$

$$k_\alpha = k_L\sqrt{1 - (k_T^2/k_L^2)\sin^2\theta_0}, \quad \theta_0 \in \langle 0, \theta_{\mathrm{MAX}}\rangle,$$

where the angle θ_{MAX} is defined by the condition $\sin\theta_{\mathrm{MAX}} = c_T/c_L$;

c) for the mode TR ($J = TR$) the quantities F_i, G_i, $k_1^{(0)}$, k are the same as for the mode SV, and

$$k_a = -ik_L \sqrt{(k_T^2/k_L^2)\sin^2\theta_0 - 1}, \quad \theta_0 \in \langle \theta_{\mathrm{MAX}}, \pi/2 \rangle; \tag{2.5}$$

d) for the Rayleigh mode ($J = R$)

$$F_1 = \frac{1}{2ik_a}, \quad F_2 = G_2 = 0, \quad G_1 = k_R(k_R^2 - k_T^2)^{-1},$$
$$k_1^{(0)} = -k_R\cos\varphi_0, \quad k_a = i\sqrt{k_R^2 - k_L^2}, \quad k_\beta = i\sqrt{k_R^2 - k_T^2}. \tag{2.6}$$

In the above expressions the pair of angles (θ_0, φ_0) defines the propagation direction of the incident wave in the particular modes (Fig. 1). For the modes SH, P these are arbitrary directions in the half-space $x_3 \geqslant 0$, while the modes SV, TR impose additional restrictions on the angle θ_0, causing a case of the incident transverse wave to be assigned either to the mode SV or to the mode TR.

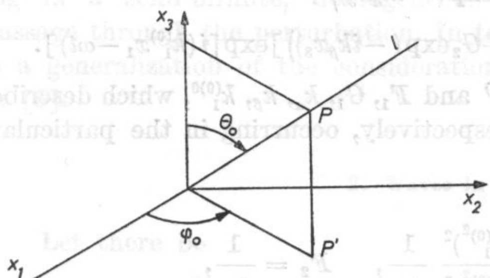

Fig. 1. The ray l represents the propagation direction for the incident waves occurring in the particular modes

The condition assumed previously for the consideration of waves with the component $k_2 = 0$ signifies that the angle φ_0 can take the values of 0 or π radians. The coupling of waves, visible in expressions (2.1)-(2.6), is a result of the existence of a free boundary plane. The coupling waves have the form of a longitudinal plane bulk wave and transverse plane bulk waves from an unbounded medium (the modes L, T) and of waves decaying exponentially with increasing distance from the boundary surface. For the boundary angles, i.e. for the rectangular incidence ($\theta_0 = 0$) and the parallel incidence ($\theta_0 = \pi/2$ and $\varphi_0 = 0$ or $\theta_0 = \pi/2$ and $\varphi_0 = 2\pi$) onto the free surface the modes show a particularly simple form, e.g. for the perpendicular incidence in the mode P only the incident and the reflected longitudinal bulk waves couple; similarly, only the incident and the reflected transverse bulk waves occur in the mode SV. It is easy to see that the variable x_2 does not occur in the expressions describing the modes and that only the mode SH has the second component of the displacement vector different from zero.

At the conclusion of this section the following notation can be introduced

$$\boldsymbol{u}^{(0,J)}(\boldsymbol{x},t) = M\boldsymbol{u}^{(0,J)}(\boldsymbol{k}_{||}^{(0)}\omega \mid x_3)\exp(i\boldsymbol{k}_{||}^{(0)}\boldsymbol{x}_{||}-\omega t),$$
$$\boldsymbol{k}_{||}^{(0)} = (k_1^{(0)},0,0), \quad \boldsymbol{x}_{||} = (x_1,x_2,0). \tag{2.7}$$

The vector $\boldsymbol{u}^{(0,J)}(\boldsymbol{k}_{||}^{(0)}\omega \mid x_3)$, describing the behaviour of modes with increasing distance from the free surface, was purposefully separated in expression (2.7), since (as will be shown in the further considerations) it components on the free surface define the scattering on perturbations. It is easy to calculate the form of this vector for the particular modes by comparing expressions (2.1), (2.2) with (2.7).

It is easy to show that for the modes P, SV propagating perpendicular to the surface S_1 the following occurs

$$u^{(0,P)}(\mathbf{0}\omega \mid 0) = 0, \quad k_1^{(0)}u^{(0,SV)}(\mathbf{0}\omega \mid 0) = 0. \tag{2.8}$$

3. Displacement field of waves scattered on the perturbation

Let the region V_1 be so perturbed that its free surface is given in the form

$$S_2 = \{\boldsymbol{x}: x_3 = F(x_1,x_2)\},$$

where

$$F(x_1,x_2) = \begin{cases} f(x_1,x_2) & \text{in the perturbed region,} \\ 0 & \text{outside the perturbed region} \end{cases} \tag{3.1}$$

i.e. the perturbation described by the function $x_3 = f(x_1, x_2)$ is a material loss of the medium. For this function we assume, in addition, that its values are low with respect to the wavelength of the wave whose propagation is considered.

This is a new elastodynamic problem for which the modes in the previous section are only a zeroth approximation to solution. The exact solution must take into consideration the changes caused by the presence of the perturbation. To the author's knowledge the effect of the perturbation on the propagating Rayleigh wave has so far been analyzed. The most important papers on this subject were [5, 11, 8]. The aim of the present paper is to determine the scattering of the other modes (i.e. the modes SH, P, SV, TR) on such perturbations.

There are the following aspects of this new elastodynamic problem. The perturbation can be regarded as a transforming structure. The case of the incident Rayleigh wave solved so for permits the statement that the perturbation transforms part of the energy of the incident wave, causing a generation of the scattered wave into bulk and Rayleigh waves (according to the notation in Fig. 2, these processes can be observed in the systems a^*-b-a, a-b-c). What

* An inderdigital transducer and a Zn0 layer permit detection and generation of Rayleigh waves in nonpiezoelectric media [5].

remains to be calculated is the problem of bulk wave scattering (using a relevant bulk wave transducer and choosing the angle θ_0 the conditions for the generation of the modes *SH*, *P*, *SV*, *TR* can be met). The solution of this problem should define, among other things, the possibilities of the transformation: bulk waves – perturbation – Rayleigh waves (according to Fig. 2 c, b, a).

In terms of the solution method this paper is a generalization of the considerations in [6].

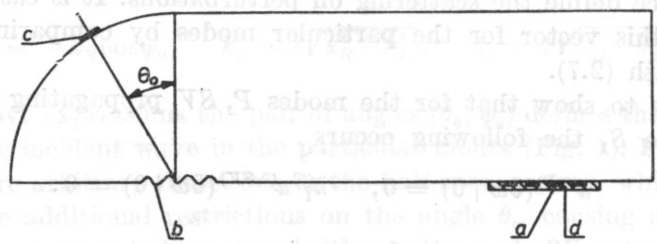

Fig. 2. An example of observation of the transforming properties for a free surface perturbation

a **– interdigital transducer,** ***b*** **– perturbation,** ***c*** **– bulk wave transducer,** ***d*** **– ZnO layer**

For this elastodynamic problem the first Born approximation for the displacement field of scattered waves can be expressed by Green functions with an expression of the form (expressions (2.12) and (2.13) in [6])

$$u^{(s)}(\boldsymbol{x}, t) = -(2\pi)^{-2} \sum_{\beta\gamma} \int d^2k \int_0^\infty dx_3' \exp(i\boldsymbol{k}_{||}\boldsymbol{x}_{||}) D_{\alpha\beta}(\boldsymbol{k}_{||}\omega \mid x_3 x_3') \times$$

$$\times \left\{ \int d^2 x_{||} \exp(-i\boldsymbol{k}_{||}\boldsymbol{x}_{||}') L^{(1)}_{\beta\gamma}(\boldsymbol{x}') \exp(i\boldsymbol{k}^{(0)}\boldsymbol{x}_{||}) \right\} u^{(0)}_{\gamma}(\boldsymbol{k}^{(0)}_{||}\omega \mid x_3') \exp(-i\omega t), \qquad (3.2)$$

where $D_{\alpha\beta}(\boldsymbol{k}_{||}\omega \mid x_3 x_3')$ are Fourier transforms of the Green function, $L^{(1)}_{\beta\gamma}(\boldsymbol{x})$ are operators defined in the Appendix, $u^{(0)}_{\gamma}(\boldsymbol{k}^0_{||}\omega \mid x_3')$ can be any solution of the wave equation in a semi-infinite medium with a free surface. Since the modes selected in section 2 form a complete system, the knowledge of the solutions for the scattered waves for these modes permits the form of scattered waves to be obtained for any wave in the half-space. In paper [6] an analytical form of the solution of equation (3.2) was derived for the case when the scattered mode is the Rayleigh wave (expressions (3.48)-(3.53) in paper [6]). This solution requires the following assumptions for the incident wave:

1) the scattered wave has the form of (2.7),
2) $u_2^{(0,J)}(\boldsymbol{k}_{||}\omega \mid x_3) = 0$,
3) $k_2^{(0)} = 0$.

The modes *P*, *SV*, *TR* satisfy conditions 1)-3), which permits generalization of the solution for the scattering of the mode *R* to include the cases when the modes *P*, *SV*, *TR*, *R* are scattered.

Some dimensionless quantities can be introduced,

$$M_1(k_{||}\omega) = \frac{k_{||}^3(2c_T^2 - c_L^2(1+\hat{k}_1^2))}{a_L(a_T^2+k^2)2c_L^2}, \quad M_3(k_{||}\omega) = \frac{k_{||}}{a_T}2\hat{k}_1\hat{k}_2,$$

$$M_2(k_{||}\omega)\frac{k_{||}(c_L^2(1+\hat{k}_1^2)-2c_T^2)}{2a_L c_L^2}, \quad M_4(k_{||}\omega) = \frac{-4a_L a_T k_{||}^2 + (a_T^2+k_{||}^2)^2}{4a_L a_T(a_T^2+k_{||}^2)}, \tag{3.3}$$

$$M_5 = \left(1-\frac{c_R^2}{2c_T^2}\right) - 5\left\{\frac{c_R^4}{c_T^4}\left(1+\frac{c_T^2}{c_L^2}\right) - \frac{c_R^2}{c_T^2}\left(9-5\frac{c_T^2}{c_L^2}\right) + 8\left(1-\frac{c_T^2}{c_L^2}\right)\right\},$$

where the wave vector of the scattered wave and the coefficients of wave decay are defined in the following way

$$\boldsymbol{k}_{||} = k_{||}(\hat{k}_1, \hat{k}_2, 0),$$

$$a_{L,T} = \begin{cases} \sqrt{k_{||}^2 - (\omega^2/c_{L,T}^2)} & \text{for } k_{||} > \omega/c_{L,T} \\ -i\sqrt{(\omega^2/c_{L,T}^2) - k_{||}^2} & \text{for } k_{||} < \omega/c_{L,T}. \end{cases} \tag{3.4}$$

The desired first Born approximation for the case when the modes P, SV, TR, R are scattered is the sum of the longitudinal and transverse bulk waves and of the Rayleigh wave

$$\boldsymbol{u}^{(S)}(\boldsymbol{x}, t) = \boldsymbol{u}^{(S,L)}(\boldsymbol{x}, t) + \boldsymbol{u}^{(S,T)}(\boldsymbol{x}, t) + \boldsymbol{u}^{(S,R)}(\boldsymbol{x}, t), \tag{3.5}$$

where the particular scattered waves have the form

$$\boldsymbol{u}^{(S,L)}(\boldsymbol{x}, t) \sim \frac{\boldsymbol{x}}{x}\left(\frac{\omega}{c_T}\right) k_1^{(0,J)} M u_1^{(0,J)}(\boldsymbol{k}_{||}^{(0)}\omega \mid 0)\hat{f}(\boldsymbol{k}_{||}^l - \boldsymbol{k}_{||}^{(0)}) \frac{\cos\theta}{2\pi i} \frac{M_1(k_{||}^l\omega)}{M_4(k_{||}^l\omega)} \times$$
$$\times \frac{\exp i\left(\dfrac{\omega}{c_L}x - \omega t\right)}{x}, \tag{3.6}$$

$$\boldsymbol{u}^{(S,T)}(\boldsymbol{x}, t) \sim \frac{M_2(k_{||}^t\omega)}{M_4(k_{||}^t\omega)}[\boldsymbol{e}_1\cos\varphi + \boldsymbol{e}_2\sin\varphi - \boldsymbol{e}_3\operatorname{tg}\theta] + M_3(k_{||}^t\omega) \times$$
$$\times[\boldsymbol{e}_1\sin\varphi - \boldsymbol{e}_2\cos\varphi]\frac{\omega}{c_T} k_1^{(0)} M u_1^{(0,J)}(\boldsymbol{k}_{||}^{(0)}\omega \mid 0)\hat{f}(\boldsymbol{k}_{||}^t - \boldsymbol{k}_{||}^{(0)}) \frac{\exp\left[i\left(\dfrac{\omega}{c_R}xi - \omega t\right)\right]}{2\pi i x}, \tag{3.7}$$

$$\boldsymbol{u}^{(S,R)}(\boldsymbol{x}, t) \sim \{[\boldsymbol{e}_1\cos\varphi + \boldsymbol{e}_2\sin\varphi][\exp(-k_R\beta_L x_3) - (1-0.5c_R^2c_T^{-2})\exp(-k_R\beta_T x_3)] +$$
$$+\boldsymbol{e}_3 i\beta_L[\exp(-k_R\beta_L x_3) - \exp(-k_R\beta_T x_3)(1-0.5c_R^2c_T^{-2}) - 1]\}(-i)(2\pi)^{-1/2}(x_{||})^{-1/2} \times$$
$$\times(\omega/c_R)^{3/2} k_1^{(0)}[M u_1^{(0,J)}(\boldsymbol{k}_{||}^{(0)}\omega \mid 0)\hat{f}(\boldsymbol{k}^R - \boldsymbol{k}_{||}^{(0)})]\exp\{i[(\pi/4) + (\omega/c_R) - \omega t]\}. \tag{3.8}$$

It should be noted that the following notation was used here

$$x = x(\sin\theta\cos\varphi,\ \sin\theta\sin\varphi,\ \cos\theta) = x_1e_1+x_2e_2+x_3e_3,$$

$$k_{\|}^{l,t} = \frac{\omega}{c_{L,T}}(\sin\theta\cos\varphi,\ \sin\theta\sin\varphi,\ 0), \tag{3.9}$$

$$k_{\|}^{R} = \frac{\omega}{c_R}(\cos\varphi,\ \sin\varphi,\ 0), \qquad \beta_{L,T} = \sqrt{1-\frac{c_R^2}{c_{L,T}^2}}\,.$$

It can be seen from the above notation that the bulk waves are spherical; the Rayleigh wave, radial; and the amplitudes of the scattered waves also depend on the direction for which the scattering is analyzed. The amplitudes of the waves generated consist of several factors:

a) $u_1^{(0,J)}(k_{\|}^{(0)}\omega \mid 0)^*$ – and, therefore, according to the considerations in the previous section, the amplitudes of the scattered waves depend on the kind of mode and are proportional to the amplitude of the incident wave; while for the incident bulk waves a change in the incidence angle also affects the magnitude of the scattered waves;

b) $f(k_{\|}-k_{\|}^{(0)})$ – the scattered waves are also defined by the shape of the perturbation;

c) $M_i(k_{\|}\omega)$ – these dimensionless functions, together with a Fourier transform of the perturbation shape function, define the angular characteristic for the scattered waves.

As was stressed above, solutions (3.6)-(3.8) are asymptotic in character.

The mode SH does not satisfy the assumptions made in paper [6] and requires additional calculation from expression (3.2). In this part of the paper, consideration will be limited to the giving of the final results (the most important stages of these tedious calculations are given in the Appendix). Some dimensionless quantities can be introduced here

$$M_1^{(SH)}(k_{\|}\omega) = \frac{i\hat{k}_1\hat{k}_2k_{\|}^3}{a_L(a_T^2+k_{\|}^2)}, \qquad M_2^{(SH)}(k_{\|}\omega) = \frac{i\hat{k}_1\hat{k}_2k_{\|}}{2a_L},$$

$$M_3^{(SH)}(k_{\|}\omega) = \frac{(\hat{k}_1^2-\hat{k}_2^2)k_{\|}}{a_T}. \tag{3.10}$$

When the quantities M_1, M_2, M_3 are replaced with the quantities

$$M_1^{(SH)},\ M_2^{(SH)},\ M_3^{(SH)} \quad \text{and} \quad u_1^{(0,J)}(k_{\|}^{(0)}\omega \mid 0) \quad \text{with}\ u_2^{(0,SH)}(k^{(0)}\omega \mid 0),$$

expressions (3.6)-(3.8) in this new form also describe the scattered waves when the mode SH is scattered. Thus, in a medium with a perturbed free surface

---

* This result can be compared to that in [12], where the form of waves scattered (in the case of the incident Rayleigh save) is defined by additional stresses occurring in the free surface.

the mode SH, as also the other modes in the half-space, becomes scattered so that the displacement field of the scattered waves is the sum of spherical (longitudinal and transverse) bulk waves and a radial Rayleigh wave. It is interesting to note that for points of the medium on the $0X_1$ axis only the amplitude of the scattered transverse wave is different from zero. This signifies that in the case of solving an analogous twodimensional problem in the scattered field of the mode SH only the transverse bulk wave occurs. This is a specific property of the mode SH which makes it different from the other modes in the semi-infinite, isotropic and linearly elastic medium.

The scattering of each mode of the complete system of modes described in section 2 is thus known. An arbitrary wave occurring in a half-space can be represented as a linear combination of modes of the complete mode system

$$\boldsymbol{u}^{(0)}(\boldsymbol{x}, t) = m_J \boldsymbol{u}^{(0,J)}(\boldsymbol{x}, t), \quad J = SH, P, SV, TR, R, \tag{3.11}$$

where m_y are expansion coefficients. Accordingly, the first Born approximation for the displacement field of scattered waves can be expressed by the formula

$$\boldsymbol{u}^{(S)}(\boldsymbol{x}, t) = m_J u^{(0,J)}(k_{\|}^{(0)}\omega \mid 0)\left\{\frac{\boldsymbol{x}}{x}\frac{\omega}{c_L}k_1^{(0)}\hat{f}(k_{\|}^{l}-\boldsymbol{k}_{\|}^{(0)})\frac{\cos\theta M_1^{(J)}(k_{\|}^{l}\omega)}{2\pi i M_4^{(J)}(k_{\|}^{l}\omega)}\times\right.$$

$$\times\frac{\exp\left[i\left(\frac{\omega}{c_T}x-\omega t\right)\right]}{x}+\frac{\omega}{c_T}k_1^{(0)}\hat{f}(\boldsymbol{k}_{\|}^{t}-\boldsymbol{k}_{\|}^{(0)})\left[\frac{M_2^{(J)}(k_{\|}^{l}\omega)}{M_4^{(J)}(k_{\|}^{l}\omega)}[\boldsymbol{e}_1\cos\varphi+\boldsymbol{e}_2\sin\varphi-\boldsymbol{e}_3\operatorname{tg}\theta]+\right.$$

$$\left.+M_3^{(J)}(k_{\|}^{t}\omega)[\boldsymbol{e}_1\sin\varphi-\boldsymbol{e}_2\cos\varphi]\right]\times\frac{\exp\left[i\left(\frac{\omega}{c_T}x-\omega t\right)\right]}{2\pi i x}+$$

$$+\left(\frac{\omega}{c_R}\right)^{3/2}k_1^{(0)}\hat{f}(k_{\|}^{R}-\boldsymbol{k}_{\|}^{(0)})M_5M_1^{(0)}(k_{\|}^{R}\omega)\frac{2\exp(i\pi/4)}{i\sqrt{2\pi}}\times$$

$$\times[\boldsymbol{e}_1\cos\varphi+\boldsymbol{e}_2\sin\varphi][\exp(-k_\beta\beta_L x_3)-\left(1-\frac{c_R^2}{2c_T^2}\right)\exp(-k_R\beta_T x_3)]+\boldsymbol{e}_3 i\beta_L\times$$

$$\left.\times\left[\exp(-k_R\beta_L x_3)-\left(1-\frac{c_R^2}{2c_T^2}\right)^{-1}\exp(-k_R\beta_T x_3)\right]\frac{\exp\left[i\left(\frac{\omega}{c_R}x-\omega t\right)\right]}{\sqrt{x_{\|}}}\right\}, \tag{3.12}$$

where

$$u^{(0,J)}(\boldsymbol{k}_{\|}^{(0)}\omega \mid 0) = \begin{cases} u_1^{(0,J)}(\boldsymbol{k}_{\|}^{(0)}\omega \mid 0), & J = P, SV, TR, R,\\ u_2^{(0,J)}(\boldsymbol{k}_{\|}^{(0)}\omega \mid 0), & J = SH,\end{cases} \tag{3.13}$$

$$M_1^{(J)}(k^{(0)}\omega) = \begin{cases} M_i(k_{\|}^{(0)}\omega), & J = P, SV, TR, R,\\ M_i^{(SH)}(k_{\|}^{(0)}\omega), & J = SH.\end{cases} \tag{3.14}$$

Expression (3.12) is valid for $k^{(S)}x \gg 1$.

4. Energy transformation on a perturbation

4.1. An acoustic Poynting vector. In considering the energy relations of waves it is convenient to use the acoustic Poynting vector $\boldsymbol{q}$. This vector is an analogue of the Poynting vector in electromagnetic theory and describes the wave power crossing a unit area. Using complex notation for the displacements $\boldsymbol{u}$ and the stress tensors T and with a harmonic dependence of waves on time, the acoustic Poynting vector defined by the relation

$$q_i' = -\frac{1}{2}\dot{u}_j^* T_{ij}, \tag{4.1}$$

is also a complex quantity, and its real part represents the time averaged power flux density for a given wave. The desired quantity is thus

$$q_i = Re\left\{-\frac{1}{2}\dot{u}_j^* T_{ij}\right\}. \tag{4.2}$$

4.2. An acoustic Poynting vector for waves incident to a perturbation. The use of definition (4.2) and of the solutions of the elastodynamic problems set in section 2 gives for the particular modes

$$q_1^{(0,SH)}\big|_{x_3=0} = \frac{1}{2}M^2\varrho\omega c_T^2 k_1^{(0)},$$

$$q_1^{(0,P)}\big|_{x_3=0} = \frac{1}{2}M^2\varrho\omega c_L^2 k_L\left\{\frac{32k_1^{(0)^3}(k_\alpha k_\beta)^2(k_\beta^2-k_\alpha^2)}{k_L[(k_\beta^2-k_1^{(0)^2})^2+4k_1^{(0)^2}k_\alpha k_\beta]^2}\right\},$$

$$q_1^{(0,SV)}\big|_{x_3=0} = \frac{1}{2}M^2\varrho\omega c_T^2 k_T\left\{\frac{16k_1^{(0)}k_\beta^2(k_\beta^2-k_1^{(0)^2})^2(k_\beta^2-k_\alpha^2)}{k_T[(k_\beta^2-k_1^{(0)^2})^2+4k_1^{(0)^2}k_\alpha k_\beta]^2}\right\},$$

$$q_1^{(0,TR)}\big|_{x_3=0} = \frac{1}{2}M^2\varrho\omega c_L^2 k_L\left\{\frac{16k_1^{(0)}k_\beta^2(k_\beta^2-k_1^{(0)^2})^2(k_\beta^2-k_\alpha^2)}{k_T[(k^2-k_1^{(0)^2})^4+(-4k_1^{(0)^2}k_\alpha k_\beta)^2]}\right\},$$

$$q_1^{(0,R)}\big|_{x_3=0} = \frac{1}{2}M^2\varrho\omega c_T^2 k_R\{2\xi_{LL}+2\xi_{LT}+2\xi_{TT}\},$$

$$q_1^{(0,J)}\big|_{x_3=0} = q_3^{(0,J)}\big|_{x_3=0} = 0, \quad J = SH, P, SV, TR, R,$$

where

$$\xi_{LL} = 2\frac{c_R^2}{2c_T^2}\left(1-\frac{c_T^2}{c_L^2}\right),$$

$$\xi_{LT} = -\left(1-\frac{c_R^2}{2c_T^2}\right)\left(2+\frac{c_R^2}{2c_T^2}-\frac{c_R^2}{c_L^2}\right)-\left(1-\frac{c_R^2}{c_L^2}\right)\left(2-\frac{c_R^2}{2c_T^2}\right)\left(1-\frac{c_R^2}{2c_T^2}\right)^{-1}, \tag{4.3}$$

$$\xi_{TT} = \left(1-\frac{c_R^2}{2c_T^2}\right)^{-1}\left[\left(1-\frac{c_R^2}{2c_T^2}\right)^3+\left(1-\frac{c_R^2}{c_T^2}\right)\right].$$

The (dimensionless) expressions in the braces result from the presence of coupling waves in the modes. It can be seen that, as expected, on the free surface energy is transfered only in the direction x_1. It is interesting to note that for the rectangular incidence with respect to the free surface in the modes SH, P, SV, no energy transport occurs in the direction x_1, either. For this reason, the time averaged acoustic Poynting vector can be calculated beforehand for the incident waves in the particular modes. For differentiation, this vector was marked with an additional dash (′).

$$\boldsymbol{q}'^{(0,P)} = \frac{1}{2} M^2 \varrho \omega c_L^2 \boldsymbol{k}_L, \quad \boldsymbol{q}'^{(0,J)} = \frac{1}{2} M^2 \varrho \omega c_T^2 \boldsymbol{k}_T, \qquad J = SH, SV, TR. \tag{4.4}$$

The physical sense of equations (4.4) is simple. They represent the power density for the incident waves in the particular modes; and at the same time represent the power density to be supplied for these modes to be generated. For the latter reason, it should be assumed that

$$\boldsymbol{q}'^{(0,R)} = \int_0^\infty \boldsymbol{q}^{(0,R)} dx_3 = \frac{1}{2} M^2 \varrho \omega\, c_T^2 \frac{\boldsymbol{k}_R}{k_R} \left\{ \frac{\xi_{LL}}{2\beta_L} + \frac{\xi_{LT}}{\beta_L + \beta_T} + \frac{\xi_{TT}}{2\beta_T} \right\}. \tag{4.5}$$

4.3. An acoustic Poynting vector for waves scattered on a perturbation. The use of definition (4.2) and of solutions (3.6)-(3.8) for large $k^{(S)} x$ (or $k_{||} x_{||}$) gives

$$\boldsymbol{q}^{(S,L)}(\boldsymbol{x}, t) = \frac{\boldsymbol{x}}{x^3} \frac{\varrho \omega^4 k_1^{(0)2}}{8\pi c_L^2} M^2 \,|\, u^{(0,J)}(\boldsymbol{k}_{||}^{(0)} \omega \,|\, 0) \hat{f}(\boldsymbol{k}_{||}^l - \boldsymbol{k}_{||}^{(0)}) \,|^2 \left| \frac{M_1^{(J)}(k_{||}^l \omega)}{M_4^{(J)}(k_{||}^l \omega)} \right|^2 \cos \theta^2, \tag{4.6}$$

$$\boldsymbol{q}^{(S,T)} = \frac{\boldsymbol{x}}{x^3} \frac{\varrho \omega^4 k_1^{(0)2}}{8\pi c_T} \,|\, M u^{(0,J)}(\boldsymbol{k}_{||}^{(0)} \omega \,|\, 0) \hat{f}(k_{||}^t - \boldsymbol{k}_{||}^{(0)}) \,|^2 + \\ + \left\{ \left| \frac{M_2^{(0,J)}(k_{||}^t)^2}{M_4^{(J)}(k_{||}^t)} \right| (1 + \operatorname{tg}^2 \theta) + |\, M_3^{(J)} \,|^2 \right\}, \tag{4.7}$$

$$\boldsymbol{q}^{(S,R)} = (\boldsymbol{e}_1 \cos\varphi + \boldsymbol{e}_2 \sin\varphi)(\pi c_R^4 x_{||})^{-1}\, 2\omega^5 c_T^2 \,|\, M u^{(0,J)}(\boldsymbol{k}_{||}^{(0)} \omega \,|\, 0) \hat{f}(k_{||}^R - \boldsymbol{k}_{||}^{(0)}) \,|^2 \times \\ \times |\, M_5 M_1^{(J)}(k_{||}^R \omega) \,|^2 \{ \xi_{LL} \exp(-2k_R \beta_L x_3) + \xi_{LT} \exp[-k_R(\beta_L + \beta_T) x_3] + \\ + \xi_{TT} \exp(-2k_R \beta_T x_3) \}. \tag{4.8}$$

Since a twodimensional Fourier transform is inversely proportional to a squared wave vector, the Poynting vector for bulk waves is proportional to ω^2, and for a radial Rayleigh wave it is proportional to ω^3, it is interesting to note that the relation

$$\boldsymbol{q}^{(S)}(\boldsymbol{x}, t) = \boldsymbol{q}^{(S,L)}(\boldsymbol{x}, t) + \boldsymbol{q}^{(S,T)}(\boldsymbol{x}, t) + \boldsymbol{q}^{(S,R)}(\boldsymbol{x}, t) \tag{4.9}$$

does not occur, since the acoustic Poynting vector also includes cross quantities describing the interference of these three waves. In practice, however, it is the quantities defined by expressions (4.6)-(4.8) that are significant, since they define the elements of the scattering matrix for a perturbation regarded as a transducer.

4.4. Power transformation on surface roughnesses. What is often essential in practice is not the absolute value of power transformed but what part of the energy of the incident wave is radiated in the form of scattered wave or waves. It is most simple to define the directional coefficient of power transformation from the wave n into the wave m as

$$\boldsymbol{KW}_{n-m} := \frac{\boldsymbol{q}^{(S,M)}}{|\boldsymbol{q}^{(0,N)}|}. \tag{4.10}$$

When, however $\boldsymbol{q}^{(0,N)}$ is replaced with $\boldsymbol{q}'^{(0,N)}$, for the reasons given in section 4.2., the directional coefficient of power transformation defines the value and direction of energy transport in the wave for the points $\boldsymbol{x}V_1$. These values are given with respect to the energy necessary for the mode n to be generated in a semi-infinite medium. Thus, definition (4.10) should finally take the form

$$\boldsymbol{KW}_{n-m} := \frac{\boldsymbol{q}^{(S,M)}}{|\boldsymbol{q}'^{(0,N)}|}. \tag{4.11}$$

In specific interesting cases of the transformation of or into Rayleigh waves, the acoustic directional power transformation coefficient is

$$\boldsymbol{KW}_{J-R} = \frac{(\boldsymbol{e}_1\cos\varphi + \boldsymbol{e}_2\sin\varphi)\,4c_T^2\omega^3}{x_{\|}\,c_R^4 c_J \pi} \,|\, u^{(0,J)}(\boldsymbol{k}_{\|}^{(0)}\omega \mid 0)\hat{f}(\boldsymbol{k}_{\|}^{l} - \boldsymbol{k}_{\|}^{(0)}) \times$$
$$\times (M_1^{(J)}(k_{\|}R_\omega)M_5|^2\{\xi_{LL}\exp(-2\beta_L k_R x_3) + \xi_{LT}\exp[-(\beta_L+\beta_T)k_R x_3] +$$
$$+\xi_{TT}\exp(-2\beta_T k_R x_3)\}, \tag{4.12}$$

where $J = SH, SV, TR, P$,

$$\boldsymbol{KW}_{R-L} = \frac{\boldsymbol{x}}{x^3}\frac{k_1^{(0)^2}\omega^3}{4c_L^2 c_T^2\pi^2}\left|\hat{f}(\boldsymbol{k}_{\|}^{l} - \boldsymbol{k}_{\|}^{(0)})\frac{M_1^{(R)}(k_{\|}^{l}\omega)}{M_1^{(R)}(k_{\|}^{l}\omega)}\right|^2\cos^2\theta\left(\frac{\xi_{LL}}{2\beta_L} + \right.$$
$$\left. + \frac{\xi_{LT}}{\beta_L+\beta_T} + \frac{\xi_{TT}}{2\beta_T}\right)^{-1}, \tag{4.13}$$

$$\boldsymbol{KW}_{R-T} = \frac{\boldsymbol{x}}{x^3}\frac{k_1^{(0)^2}\omega^3}{4c_T^3\pi^2}\;|\hat{f}(\boldsymbol{k}_{\|}^{t} - \boldsymbol{k}_{\|}^{(0)})|^2\left\{\left|\frac{M_2^{(R)}(k_{\|}^{t}\omega)}{M_4^{(R)}(k_{\|}^{t}\omega)}\right|^2 \times\right.$$
$$\left.\times(1+\mathrm{tg}^2\theta) + |M_3^{(R)}(k_{\|}^{t}\omega)|^2\right\}\left\{\frac{\xi_{LL}}{2\beta_L} + \frac{\xi_{LT}}{\beta_L+\beta_T} + \frac{\xi_{TT}}{2\beta_T}\right\}, \tag{4.14}$$

$$KW_{R-R} = \frac{(e_1\cos\varphi + e_2\sin\varphi)\,4\omega^4}{x_{||}c_R^4\pi}\,|f(k_{||}^R - k_{||}^R)\,M_1^{(R)}(k_{||}^R\omega)\,M_5\,|^2 \times$$
$$\times\left(\frac{\xi_{LL}}{2\beta_L} + \frac{\xi_{LT}}{\beta_L+\beta_T} + \frac{\xi_{TT}}{2\beta_T}\right)^{-1} \xi_{LL}\exp(-2\beta_L k_R x_3) + \xi_{LT}\exp[-(\beta_L+\beta_T)k_R x_3] +$$
$$+\xi_{TT}\exp(-2\beta_T k_R x_3). \qquad (4.15)$$

The expressions given above permit the perturbation of the free surface to be regarded as a transducer with five inputs, corresponding to five modes from the unperturbed medium, and three outputs, corresponding to three kinds of scattered waves. The elements of the scattering matrix of such a transducer (giving the magnitude of power obtained at the outputs after supplying an arbitrary mode to the input) are equal to the directional power transformation coefficients calculated in section 4.4. This transducer involves the following transformations:

1) Rayleigh waves into bulk waves (proportional to ω),
2) bulk waves into Rayleigh waves (proportional to ω^{-1}),
3) Rayleigh waves into Rayleigh waves (proportional to ω^0),
4) bulk waves into bulk waves (proportional to ω^0).

The first two transformations are particularly interesting in practice. Transducers for which only these two transformations are considered are called surface-structure transducers [1]. It is interesting to note that when a specific structure is considered (Fig. 1), the quantities $x_{||}$, x are constant and only one mode of the modes SV and TR exists. Such a transducer has thus four inputs and three outputs, and the elements of the scattering matrix are proportional to $\pm\,\omega$. For a twodimensional problem, in view of the lack of scattering of the mode SH into a Rayleigh wave, the matrix of the surface-structure transducer has only three inputs and three outputs. This agrees with the results of paper [1].

5. The effect of the shape of a perturbation on the magnitude of power transformed

The directional power transformation coefficient is proportional to a Fourier transform of the perturbation shape function. This is a general conclusion from expressions (4.12)-(4.15). Very interesting results can, however, be obtained from analysis of a certain class of the perturbation shape function, defined as

$$f(x_1, x_2) = f(x_1) = f_0(x_1) + f_0(x_1+2L) + \ldots + f_0(x_1+2Lm), \qquad (5.1)$$

where $f_0(x_1)$ describes a perturbation over a rectangular area of dimensions $2L\times L_2$. Thus, $f(x_1)$ corresponds to a periodic system of grooves of arbitrary shape, parallel to the $0X_2$ axis. In practice, such a character can be observed in surface-structure transducers, bulk wave resonators.

The values of the Fourier transform $\hat{f}(k_{\|}^{(S)}-k_{\|}^{(0)'})$ can now be analyzed for the points x belonging to the plane $x_1 0 X_2$ (in the spherical coordinate system, this signifies a restriction of the angles φ to a value of zero or π radians)

$$\hat{f}(k_{\|}^{(S)}-k_{\|}^{(0)}) = \sum_{n=0}^{m} L_2 \exp[i(k_1^{(S)}-k_1^{(0)})2Ln]\hat{f}_0(k_1^{(S)}-k_1^{(0)})$$

$$= L_2 \exp[i(k_1^{(S)}-k_1^{(0)})Lm]\frac{\sin(k_1^{(S)}-k_1^{(0)})Lm}{\sin k_1^{(S)}-k_1^{(0)}L}\hat{f}_0(k_1^{(S)}-k_1^{(0)}). \tag{5.2}$$

Consideration of this result in expressions (3.12) and (4.6)-(4.8) leads to the conclusion that the resultant scattered wave is the sum of waves scattered on subsequent grooves; and the scattered power is the power of the resultant scattered wave. The latter statement also signifies that the power radiated on a system of grooves can be expressed with the power radiated on a single groove, modulated by the expression

$$W = \frac{\sin(k_1^{(S)}-k_1^{(0)})Lm}{\sin(k_1^{(S)}-k_1^{(0)})L}. \tag{5.3}$$

This expression has a maximum when the following condition is satisfied,

$$(k_1^{(S)}-k_1^{(0)})L = l\pi, \quad l = 0, \pm 1, \pm 2, \ldots \tag{5.4}$$

These conditions can be written otherwise as

a) for the scattering of Rayleigh waves into bulk waves

$$k_1^{(S)} = k_n \sin\theta\cos\varphi, \quad k_1^{(0)} = -k_R \cos\varphi_0, \quad n = L, T,$$

$$L = \frac{\pi l c_R}{\omega}\left(\frac{c_R}{c_n}\sin\theta\cos\varphi + \cos\varphi_0\right)^{-1}; \tag{5.5}$$

b) for the scattering of the modes SH, P, SV, TR, into Rayleigh waves

$$L = \frac{\pi l c_R}{\omega}\left(\frac{c_R}{c_n}\sin\theta_0\cos\varphi_0 + \cos\varphi\right)^{-1}, \tag{5.6}$$

where ω is the frequency of the incident waves, and l is such that for given angles the period L is positive. At the same time, for a stable L expressions (5.5) and (5.6) define the angles at which the value of W is maximum. This is a result of the interference of waves generated on subsequent grooves. For perturbations of a periodic, large number of grooves, these are, in practice, the only directions in which energy is radiated. These conditions provide a design for the construction of transforming structures for which the power transformation coefficient is as large as possible. It is interesting to note that there is a minimum L

$$L_{\min} = \lambda_R\left(1+\frac{\lambda_R}{\lambda_n}\right)^{-1}. \tag{5.7}$$

This signifies that for $L < L_{\min}$ no energy transformation occurs in the surface-structure transducer. This condition is used in devices where this transformation is undesired [9].

6. Conclusion

This paper considered the scattering of acoustic waves (propagating in a semi-infinite medium) on perturbations of a free surface under the assumptions that 1) the function describing the shape of a perturbation takes low values with respect to the wavelength of a propagating wave, and that 2) the ratio of power transformed to the power of the incident wave is considerably lower than unity. This perturbation transforms part of the incident energy, causing generation of a scattered wave in the form of a radial Rayleigh wave and spherical bulk waves: a longitudinal wave and a transverse one. It is interesting to note that this solution is asymptotic. The amplitudes of waves generated depend on the kind of mode, the incidence angle of the mode (for bulk modes), the shape of the perturbation and the amplitude of the incident wave. For a perturbation being a periodic function, relative to one of the coordinates, the scattering of waves of stable frequency shows additional properties: 1) radiation only occurs in some directions, 2) for a period less than some $L_{\min}$, there is no scattering of Rayleigh waves into bulk waves or of bulk waves into Rayleigh waves.

In practice, these perturbations can be regarded as transducers in which the following transformations occur: 1) Rayleigh waves into bulk waves, 2) bulk waves into Rayleigh waves, 3) Rayleigh waves into Rayleigh waves, 4) bulk waves into bulk waves. In these transformations the power ratio of waves generated to the incident waves is proportional, respectively, to the powers of frequency — 1) + [the first, 2) — the first, 3) the zeroth. Additional properties of structures with periodic perturbations permit the designing of optimum transformation.

Acknowledgement. This paper was written in the course of the author's doctoral studies at the Institute of Fundamental Technological Research. The author wishes to express his gratitude to prof. I. Malecki and Prof. A. Opilski for their advice.

References

[1] I. D. Akhromeyeva, V. V. Krilov, *Preobrazovanye voln Releya v obyemniye na lokalnikh defektakh poverkhnosti,* Akusticheskiy Zhurnal, **XXIII**, 4, 510-516 (1977).

[2] K. Dransfeld, E. Salzmann, *Excitation, detection and attenuation of high frequency elastic waves,* Physical Acoustics, v. VII, W. P. Mason Academic Press, New York and London 1970.

[3] H. Ezawa, *Phonons in a half space*, Annals of Physics, **67**, 438-460 (1971).

[4] R. F. Humphreyes, E. A. Ash, *Acoustic bulk-surface-wave transducer*, Electronics Letters, **12**, 13, 175-176 (1969).

[5] G. S. Kino, R. S. Wagers, *Theory of interdigital couplers on nonpiezoelectric substrates*, Journal of Applied Physics, **44**, 4, 1480-1488/19.

[6] A. A. Maradudin, D. L. Mills, *The attenuation of Rayleigh surface waves by surface roughness*, Annals of Physics, 100, 262-309 (1976).

[7] A. Ronnekleiv, H. J. Shaw, J. Souquet, *Grating acoustic scanners*, Applied Physics Letters, **28**, 7, 361-361 (1976).

[8] A. Ronnekleiv, H. J. Shaw, J. Souquet, *Experimental acoustic-surface wave-to-bulk-wave scattering by grooves*, Electronics Letters, **12**, 11, 267-269 (1976).

[9] A. Ronnekleiv, H. J. Souquet, *On the theory of acoustic surface wave to bulk wave scattering by grooves*, Journal of Applied Physics, **47**, 10, 4422-4425 (1976).

[10] P. V. H. Sabine, *Rayleigh – wave propagation on a periodically roughened surface*, Electronics Letters, **6**, 6, 149-151 (1970).

[11] H. S. Tuan, *Acoustic-surface-wave scattering at a region with material perturbation*, Journal of Applied Physics, **47**, 4, 1248-1252 (1976).

[12] H. S. Tuan, *On bulk waves excited at a groove by Rayleigh waves*, Journal of Applied Physics, **46**, 1, 36-41 (1975).

[13] M. Yamanishi, M. Ameda, T. Kawamura, *Generation of 880 MHz surface acoustic waves by transduction from bulk wave using corrugation greating on GaAs*, Electronics Letters, **12**, 13, 317-318 (1976).

Received on October 3, 1979 ; revised version on June 10, 1981.

Appendix

Integral (3.2) can be calculated for the case of the scattering of the mode SH. According to expression (2.1), only the second component of the displacement vector is different from zero, and the desired solution takes thus the form

$$u_a(\boldsymbol{x}, t) = \exp(-i\omega t) \sum_{\beta} \int d^2k_{||} (2\pi)^{-2} \int_0^{\infty} dx_3' \exp(i\boldsymbol{k}_{||}\boldsymbol{x}_{||}) D_{a\beta}(\boldsymbol{k}_{||}\omega \,|\, \times$$

$$\times x_3 x_3') \int d^2x_{||}' \exp(-i\boldsymbol{k}_{||}\boldsymbol{x}_{||}) L^{(1)}_{\beta 2}(\boldsymbol{x}') \exp(i\boldsymbol{k}^{(0)}_{||}\boldsymbol{x}'_{||}) u_2^{(0,SH)}(\boldsymbol{k}^{(0)}_{||}\omega \mid 0). \quad \text{(A1)}$$

The operators $L^{(1)}_{\beta\gamma}(\boldsymbol{x})$ are defined as

$$L^{(1)}_{\beta\gamma}(\boldsymbol{x}) = \frac{1}{\varrho} \sum_{au} \frac{\partial c^{(1)}_{\beta a \gamma u} \partial}{\partial x_a \partial x_u} + \frac{1}{\varrho} \sum_{au} c^{(1)}_{\beta a \gamma u} \frac{\partial^2}{\partial x_a \partial x_u}, \quad \text{(A2)}$$

and the elastic constants are defined as

$$c_{\beta a \gamma u}(\boldsymbol{x}) = -f(x_1, x_2) c_{\beta a \gamma u}, \quad \text{(A3)}$$

where $x_3 = f(x_1, x_2)$ is a function of perturbation shape. The necessary operators $L^{(1)}_{\beta 2}(\boldsymbol{x})$ are, respectively,

$$L^{(1)}_{12}(\boldsymbol{x}) = -c_T^2 \delta(x_3) \frac{\partial f(x_1, x_2)}{\partial x_2} \frac{\partial}{\partial x_2},$$

$$L^{(1)}_{22}(\boldsymbol{x}) = -c_T^2 \delta(x_3) \left\{ \frac{\partial f}{\partial x_1} \frac{\partial}{\partial x_1} + f\left(\frac{\partial^2}{\partial x_1^2} + \frac{\partial^2}{\partial x_3^2} \right) \right\} - c_T^2 \delta'(x_3) f \frac{\partial}{\partial x_3}, \tag{A4}$$

$$L^{(1)}_{32}(\boldsymbol{x}) = -c_T^2 \delta(x_3) \frac{\partial f}{\partial x_2} \frac{\partial}{\partial x_3}.$$

Using (A4), equation (A1) becomes finally

$$u_a^{(S)}(\boldsymbol{x}, t) = \exp(-i\omega t) \int d^2 k_{||} (2\pi)^{-2} i k_1^{(0)} \hat{f}(\boldsymbol{k}_{||} - \boldsymbol{k}_{||}^{(0)}) \{k_2 D_{a1} + k_1 D_{a2}\} \exp(i \boldsymbol{k}_{||} \boldsymbol{x}_{||}). \tag{A5}$$

Substitution of the explicit form of the Green function for a semiinfinite region gives the displacement vector for scattered waves in the form

$$\boldsymbol{u}^{(S)}(\boldsymbol{x}, t)\exp(i\omega t) = \int d^2 k_{||} \frac{u^{(l)}(\boldsymbol{k}_{||} \boldsymbol{k}_{||}^{(0)} \omega)}{4\pi^2 r_+(k_{||}\omega)} \left[\boldsymbol{e}_1 k_1 + \boldsymbol{e}_2 k_2 + \boldsymbol{e}_3 i \frac{a_L}{k_{||}} \right] \times$$
$$\times \exp(-a_L x_3 + i \boldsymbol{k}_{||} \boldsymbol{x}_{||}) + \int d^2 k_{||} \frac{u^{(ta)}(\boldsymbol{k}_{||} \boldsymbol{k}_{||}^{(0)} \omega)}{4\pi^2 r_+(k_{||}\omega)} \left[\boldsymbol{e}_1 k_1 + \boldsymbol{e}_2 k_2 + \boldsymbol{e}_3 i \frac{k_{||}}{a_L} \right] \times$$
$$\times \exp(-a_T x_3 + i \boldsymbol{k}_{||} \boldsymbol{x}_{||}) + \int d^2 k_{||} (2\pi)^{-2} u^{(tb)}(\boldsymbol{k}_{||} \boldsymbol{k}_{||}^{(0)} \omega) [\boldsymbol{e}_1 k_2 - \boldsymbol{e}_2 k_1] \times$$
$$\times \exp(-a_T x_3 + i \boldsymbol{k}_{||} \boldsymbol{x}_{||}), \tag{A6}$$

where

$$r_+(\boldsymbol{k}_{||}\omega) = \frac{4 a_T c_T^2 \boldsymbol{k}^2 + (\omega^2 - 2 c_T \boldsymbol{k}_{||}^2)(a_T^2 - \boldsymbol{k}_{||}^2)}{4 a_T a_L (\omega^2 - 2 c_T^2 \boldsymbol{k}_{||}^2)},$$

$$u^{(l)}(\boldsymbol{k}_{||} \boldsymbol{k}_{||}^{(0)} \omega) = M u_2^{(0,SH)}(\boldsymbol{k}_{||}^{(0)} \omega \mid 0) \hat{f}(\boldsymbol{k}_{||} - \boldsymbol{k}_{||}^{(0)}) \frac{i k_1^{(0)} \hat{k}_1 k_2 k_{||}^3}{a_L (a_T^2 + k_{||}^2)},$$

$$u^{(ta)}(\boldsymbol{k}_{||} \boldsymbol{k}_{||}^{(0)} \omega) = M u_2^{(0,SH)}(\boldsymbol{k}_{||}^{(0)} \omega \mid 0) \hat{f}(\boldsymbol{k}_{||} - \boldsymbol{k}_{||}^{(0)}) \frac{i k_1^{(0)} \hat{k}_1 \hat{k}_2 k_{||}}{2 a_L},$$

$$u^{(tb)}(\boldsymbol{k}_{||} \boldsymbol{k}_{||}^{(0)} \omega) = M u_2^{(0,SH)}(\boldsymbol{k}_{||}^{(0)} \omega \mid 0) \hat{f}(\boldsymbol{k}_{||} - \boldsymbol{k}_{||}^{(0)}) \frac{i k_1 k_{||} (\hat{k}_1^2 - \hat{k}_2^2)}{a_L}.$$

The integrals occurring in expression (A6) are those of types considered in [6]. An asymptotic form of the solution of these integrals has already been given in the main text of the paper.

ARCHIVES OF ACOUSTICS
7, 1, 61 – 70 (1982)

ULTRASONIC WAVE PROPAGATION IN A LAYERED MEDIUM UNDER DIFFERENT BOUNDARY CONDITIONS

ALEKSANDER PILARSKI

Institute of Fundamental Technological Research (00-049 Warsaw, ul. Świętokrzyska 21)

This paper presents an analysis of the possibility of using the phase velocity measurements of surface or plate waves for the evaluation of the adhesive bond strength, i.e. of the adhesion degree in layered joints. Dispersive curves are determined for phase velocities in layer on base and layer on layer systems with two kinds of boundary conditions, i.e. welded and smooth ones, by numerical solutions of the characteristic equations. The procedure of deriving these equations for any number of layers is given.

1. Introduction

Ultrasonic methods using the phenomenon of ultrasonic wave propagation in elastic layered media area can be used not only for detecting the unbounded but also for evaluating the bond strength [1].

Seismologists and geophysicists have long been interested in elastic waves propagating in layered media [2-4]. Waves propagating parallel to boundary surfaces in layered media can, for the sake of simplicity and by analogy to nondestructive testing terminology, be called below surface waves in the case of a layer, or layers on a base, and plate waves in the case of one or more solid layers. A base means a solid medium of thickness exceeding several times the wavelength of a surface mode, while a solid medium of thickness comparable with the wavelength of a surface mode is regarded as a layer. For example, a metal sheet glued to thick rubber involves surface waves, while a simple lap adhesive joint involves plate waves. Both can, however, have a common mathematical approach (cf. next section).

The previous attempts at using surface waves [5] or plate waves [6] for evaluating the bond strength of adhesive joints consisted in the measurements of decay in these waves after they have passed through a controlled section. The aim of the present paper is to analyze the possibility of evaluating the adhesion degree in layered joints made by different techniques, on the basis of velocity measurements of waves propagating along the connection. For this purpose dispersive curves of phase velocity can be determined numerically for different boundary conditions. The knowledge of these characteristics permits not only the estimation of the sensitivity of the acoustic parameter, i.e. the phase velocity, to changes in the strength of a connection, but also makes it easier to conduct a purposive experimental research.

2. Characteristic equation

Mathematically, this problem can be formulated in the following way for flat parallel layers (homogeneous, isotropic and ideally elastic media). The solutions of the twodimensional wave equations [7] are sought

$$\nabla^2\varphi = \frac{1}{c_L^2}\varphi_{,tt}, \quad \nabla^2\psi = \frac{1}{c_T^2}\psi_{,tt}, \quad \nabla^2 = \partial_{,xx}+\partial_{,zz}; \tag{1}$$

with the assumption that their solutions, i.e. their scalar potentials φ and ψ are sought in the form

$$\varphi(x,z,t) = \varphi^*(z)\exp[ik(x+ct)], \quad \psi(x,z,t) = \psi^*(z)\exp[ik(x+ct)]. \tag{2}$$

This signifies that the wave is harmonic in time and moves in the negative direction of the x axis. In these formulae c_L and c_T are the velocities of longitudinal and transverse waves, respectively, while k is the wave number $k = \omega/c$. Insertion of formulae (2) into (1) gives the simple differential equations

$$(\partial_{,zz}-k^2s^2)\varphi^* = 0, \quad (\partial_{,zz}-k^2q^2)\psi^* = 0, \tag{3}$$

where

$$s = [1-(c/c_L)^2]^{1/2}, \quad q = [1-(c/c_T)^2]^{1/2}. \tag{4}$$

Therefore, the general solution of equations (1) for the mth layer (Fig. 1) can be given in the form

$$\varphi_m = [A_{4m-3}\cosh(ksz)+A_{4m-2}\sinh(ksz)]\exp[ik(x+ct)], \tag{5}$$

$$\psi_m = [A_{4m-1}\cosh(kqz)+A_{4m}\sinh(kqz)]\exp[ik(x+ct)] \tag{6}$$

while in the half-space (medium $n+1$) the solution of equations (1) can be given as

$$\varphi_{n+1} = A_{4n+1}\exp(-ksz)\exp[ik(x+ct)], \tag{7}$$

$$\psi_{n+1} = A_{4n+2}\exp(-kqz)\exp[ik(x+ct)]. \tag{8}$$

The displacements u and w and also the stresses σ_{zz} and σ_{xz} are related to the functions φ and ψ by the relations

$$u = \varphi_{,x} - \psi_{,z}, \quad w = \varphi_{,z} + \psi_{,x}, \tag{9}$$

$$\sigma_{zz} = G[(c_L/c_T)^2 - 2]\varphi_{,xx} + G(c_L/c_T)^2\varphi_{,zz} + 2G\psi_{,xz}, \tag{10}$$

$$\sigma_{xz} = 2G\varphi_{,xz} - G\psi_{,zz} + G\psi_{,xx}. \tag{11}$$

Insertion of (5) and (6) and also of (7) and (8) into (9)-(11) gives

$$u_m = \{ik[A_{4m-3}\cosh(ks_m z) + A_{4m-2}\sinh(ks_m z)] - \\ -kq_m[A_{4m-1}\sinh(kq_m z) + A_{4m}\cosh(kq_m z)]\}\exp[i(\omega t + kx)], \tag{12}$$

$$w_m = \{ks_m[A_{4m-3}\sinh(ks_m z) + A_{4m-2}\cosh(ks_m z)] + \\ +ik[A_{4m-1}\cosh(kq_m z) + A_{4m}\sinh(kq_m z)]\}\exp[i(\omega t + kx)], \tag{13}$$

$$(\sigma_{zz})_m = \{G_m k^2 r_m[A_{4m-3}\cosh(ks_m z) + A_{4m-2}\sinh(ks_m z)] + \\ +i2G_m k^2 q_m[A_{4m-1}\sinh(kq_m z) + A_{4m}\cosh(kq_m z)]\}\exp[i(\omega t + kx)], \tag{14}$$

$$(\sigma_{xz})_m = \{i2G_m k^2 s_m[A_{4m-3}\sinh(ks_m z) + A_{4m-2}\cosh(ks_m z)] - \\ -G_m k^2 r_m[A_{4m-1}\cosh(kq_m z) + A_{4m}\sinh(kq_m z)]\}\exp[i(\omega t + kx)], \tag{15}$$

$$u_{n+1} = [A_{4n+1}ik\exp(-ks_{n+1}z) + A_{4n+2}kq_{n+1}\exp(-kq_{n+1}z)]\exp[i(\omega t + kx)], \tag{16}$$

$$w_{n+1} = [-A_{4n+1}ks_{n+1}\exp(-ks_{n+1}z) + A_{4n+2}ik\exp(-kq_{n+1}z)]\exp[i(\omega t + kx)], \tag{17}$$

$$(\sigma_{zz})_{n+1} = [A_{4n+1}G_{n+1}k^2 r_{n+1}\exp(-ks_{n+1}z) - A_{4n+2}2G_{n+1}ik^2 q_{n+1}\exp(-kq_{n+1}z) \times \\ \times \exp[i(\omega t + kx)], \tag{18}$$

$$(\sigma_{xz})_{n+1} = [-A_{4n+1}2G_{n+1}ik^2 s_{n+1}\exp(-ks_{n+1}z) - A_{4n+2}G_{n+1}k^2 r_{n+1}\exp(-kq_{n+1}z)] \times \\ \times \exp[i(\omega t + kx)]. \tag{19}$$

In these formulae the following quantity was introduced

$$r = 2 - (c/c_T)^2. \tag{20}$$

Subsequently, using the relevant boundary conditions for the coordinate $z_0 = -(h_1 + \ldots + h_m + \ldots + h_n), \ldots, z_m = -(h_{m+1} + \ldots + h_n), \ldots, z_n = 0$ given in Table 1, a system of homogeneous linear equations can be obtained,

$$\sum_{j=1}^{4n+2(4n)} a_{ij}A_j = 0 \quad [i = 1, 2, \ldots, (4n), \ldots, (4n+2)], \tag{21}$$

where for n layers on base there are $(4n+2)$ equations with $(4n+2)$ unknowns and for n layers $(4n)$ equations with $(4n)$ unknowns.

System (21) has a non-trivial solution when

$$D_n = \det[a_{ij}] = 0. \tag{22}$$

The determinant D_n is of order $(4n+2)$ or $(4n)$. The matrix $[a_{ij}]$ can be divided into rectangular matrices in the following way

$$[a_{ij}] = \begin{pmatrix} [a_{ij}]_0 & [0] & & \\ [0] & [a_{ij}]_m & [0] & \\ & [0] & [a_{ij}]_n & \end{pmatrix}, \tag{23}$$

where the particular matrices result from the assumption of relevant boundary conditions (Table 1).

Table 1. Boundary conditions for the particular matrices

Matrices		Boundary conditions	
symbol	dimensions	welded	smooth
free surface $[a_{ij}]_0$	2×4	$(\sigma_{xz})_1 = (\sigma_{zz})_1 = 0$	$(\sigma_{xz})_1 = (\sigma_{zz})_1 = 0$
mth interface $[a_{ij}]_m$	4×8	$(\sigma_{xz})_m = (\sigma_{xz})_{m+1}$ $(\sigma_{zz})_m = (\sigma_{zz})_{m+1}$ $u_m = u_{m+1}$ $w_m = w_{m+1}$	$(\sigma_{xz})_m = 0$ $(\sigma_{zz})_m = (\sigma_{zz})_{m+1}$ $(\sigma_{xz})_{m+1} = 0$ $w_m = w_{m+1}$
nth interface $[a_{ij}]_n$	4×6	$(\sigma_{xz})_n = (\sigma_{xz})_{n+1}$ $(\sigma_{zz})_n = (\sigma_{zz})_{n+1}$ $u_n = u_{n+1}$ $w_n = w_{n+1}$	$(\sigma_{xz})_n = 0$ $(\sigma_{zz})_n = (\sigma_{zz})_{n+1}$ $(\sigma_{xz})_{n+1} = 0$ $w_n = w_{n+1}$
free surface $[a_{ij}]_n$	2×4	$(\sigma_{xz})_n = (\sigma_{zz})_n = 0$	$(\sigma_{xz})_n = (\sigma_{zz})_n = 0$

For the purposes of the present work, after NICKERSON's suggestion [8], boundary conditions can be divided into welded and smooth. The welded conditions assume a continuity of displacements and stresses, both normal and tangent, corresponding to an ideal connection of two solids (welded contact). The smooth conditions allow a decrease in stresses tangent to boundary conditions, i.e. correspond to smooth contact. Such a case can be conceived, after ACHENBACH [9], as two solids separated by an inviscid liquid of infinitely small thickness. It can be assumed that real bonds of different adhesion degree fall between these two extreme cases of boundary conditions.

Therefore, using formulae (12)-(20) and Table 1, a determinant can be determined for any layered joint with different boundary conditions. Equating this determinant to zero leads to a characteristic equation from which the phase velocity can be determined for predetermined values of the density ϱ, the modulus of longitudinal elasticity E, the modulus of transverse elasticity G, thicknesses of the particular layers and frequency.

For example, for a single layer ($n = 1$), from Table 1 boundary conditions are chosen only for free surfaces, giving the determinant $\det[a_{ij}]$ of the fourth order, which when equated to zero becomes a characteristic equation for the problem solved by LAMB [10].

From the point of view of the evaluation of adhesion in layered joints, the following cases are of most interest here: layer on base, layer on layer, two layers on base and three layers. The first two cases correspond to bimetals, while the other two to adhesive bonded joints or soldered joints.

The present paper gives a schematic procedure for determination of a characteristic equation in the case of a flat parallel layer on base and of two layers, for two kinds of boundary conditions. Using the KEILIS-BOROK [4] notation these equations can be written as

$$D_1^{(1,2)} = 0 \quad \text{and} \quad D_2^{(1,2)} = 0,$$

where the lower index denotes the number of layers, the index in brackets the subsequent layers or, possibly, the base, while D is the determinant (see equation (22)).

3. Layer on base $[D_1^{(1,2)} = 0]$

(a) *Welded contact.* The starting point for derivation of the characteristic equation in the case of layer on base for welded boundary conditions is, according to Table 1, the six boundary conditions

$$(\sigma_{xz})_1 = (\sigma_{zz})_1 = 0 \tag{24}$$

for $z = z_0 = -h$;

$$(\sigma_{xz})_1 = (\sigma_{xz})_2, \quad (\sigma_{zz})_1 = (\sigma_{zz})_2, \tag{25}$$

$$u_1 = u_2, \quad w_1 = w_2 \tag{26}$$

for $z = z_1 = 0$.

Writing the stresses and displacements occurring in equations (24)-(26) by means of formulae (12)-(20) gives a system of six homogeneous equations relative to the six unknowns $A_1, A_2, \ldots, A_6$. By forming the determinant from indices of the unknowns and equating it to zero, after slight transformations [11], the characteristic equation can be obtained

$$\begin{vmatrix} -2s_1\sinh S_1 & 2\cosh S_1 & -r_1\cosh Q_1 & r_1\dfrac{\sinh Q_1}{q_1} & 0 & 0 \\ r_1\cosh S_1 & -r_1\dfrac{\sinh S_1}{s_1} & 2q_1\sinh Q_1 & -2\cosh Q_1 & 0 & 0 \\ 0 & 2 & -r_1 & 0 & 2gs_2 & gr_2 \\ r_1 & 0 & 0 & -2 & -gr_2 & -2gq_2 \\ 1 & 0 & 0 & -1 & -1 & -q_2 \\ 0 & 1 & -1 & 0 & s_2 & 1 \end{vmatrix} = 0, \tag{27}$$

where for the sake of brief notation new symbols were introduced; namely

$$S_1 = -ks_1z_0, \quad Q_1 = -kq_1z_0, \quad g = G_2/G_1. \tag{28}$$

(b) *Smooth contact.* In this case the starting point for derivation of the characteristic equation can be, according to Table 1, the following six boundary conditions

$$(\sigma_{xz})_1 = (\sigma_{zz})_1 = 0 \tag{29}$$

for $z = z_0 = -h$;

$$(\sigma_{xz})_1 = (\sigma_{xz})_2 = 0, \tag{30}$$

$$(\sigma_{zz})_1 = (\sigma_{zz})_2, \quad w_1 = w_2 \tag{31}$$

for $z = z_1 = 0$.

By a procedure analogous to point *a*), after transformations, the characteristic equation can be obtained

$$\begin{vmatrix} -2s_1\sinh S_1 & 2\cosh S_1 & -r_1\cosh Q_1 & r_1\dfrac{\sinh Q_1}{q_1} & 0 & 0 \\ r_1\cosh Q_1 & -r_1\dfrac{\sinh S_1}{s_1} & 2q_1\sinh Q_1 & -2\cosh Q_1 & 0 & 0 \\ 0 & 2 & -r_1 & 0 & 0 & 0 \\ r_1 & 0 & 0 & -2 & -gr_2 & -2gq_2 \\ 0 & 0 & 0 & 0 & 2s_2 & r_2 \\ 0 & 1 & -1 & 0 & s_2 & 1 \end{vmatrix} = 0, \tag{32}$$

4. Layer on laxer $[D_2^{(1,2)} = 0]$

The same procedure as in point 3a gives characteristic equations whose left sides, in view of eight boundary conditions (two for each of free surfaces and four for the interface), are determinants of dimensions 8×8. A diagram of the left sides of these equations, with plotted zero elements and those characteristic of a given type of boundary conditions, is shown in Fig. 2. There is the following set of the particular elements:

— The elements a_{ij} common to welded and smooth boundary conditions:

$a_{11} = -2s_1\sinh S_1, \quad a_{12} = 2\cosh S_1, \quad a_{13} = -r_1\cosh Q_1, \quad a_{14} = r_1\sinh Q_1/q_1,$
$a_{21} = r_1\cosh S_1, \quad a_{22} = -r_1\sinh S_1/s_1, \quad a_{23} = 2q_1\sinh Q_1, \quad a_{24} = -2\cosh Q_1,$
$a_{31} = -2s_1\sinh \bar{S}_1, \quad a_{32} = 2\cosh \bar{S}_1, \quad a_{33} = -r_1\cosh \bar{Q}_1, \quad a_{34} = r_1\sinh \bar{Q}_1/q_1,$
$a_{41} = r_1\cosh \bar{S}_1, \quad a_{42} = -r_1\sinh \bar{S}_1/s_1, \quad a_{43} = 2q_1\sinh \bar{Q}_1, \quad a_{44} = -2\cosh \bar{Q}_1,$
$a_{45} = -r_2g\cosh S_2, \quad a_{46} = r_2g\sinh S_2/s_2, \quad a_{47} = -2gq_2\sinh Q_2, \quad a_{48} = 2g\cosh Q_2,$
$a_{61} = -s_1\sinh \bar{S}_1, \quad a_{62} = \cosh \bar{S}_1, \quad a_{63} = -\cosh \bar{Q}_1, \quad a_{64} = \sinh \bar{Q}_1/q_1,$
$a_{65} = s_2\sinh S_2, \quad a_{66} = -\cosh S_2, \quad a_{67} = \cosh Q_2, \quad a_{68} = -\sinh Q_2/q_2,$
$a_{75} = a_{78} = a_{86} = a_{87} = 0, \quad a_{76} = 2, \quad a_{77} = -r_2, \quad a_{85} = r_2, \quad a_{88} = -2.$

– The elements a_{ij} characteristic of welded boundary conditions:
$a_{35} = 2s_2 g \sinh S_2$, $a_{36} = -2g \cosh S_2$, $a_{37} = r_2 g \cosh Q_2$, $a_{38} = -r_2 g \sinh Q_2/$ $/q_2$, $a_{51} = \cosh \overline{S}_1$, $a_{52} = -\sinh \overline{S}_1/s_1$, $a_{53} = q_1 \sinh \overline{Q}_1$, $a_{54} = -\cosh \overline{Q}_1$, $a_{55} = -\cosh S_2$, $a_{56} = \sinh S_2/s_2$, $a_{57} = -q_2 \sinh Q_2$, $a_{58} = \cosh Q_2$.

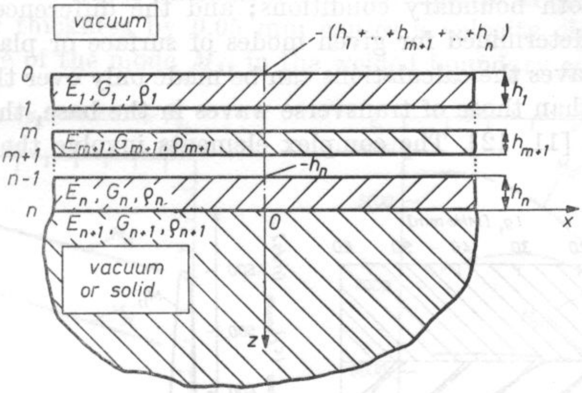

Fig. 1. A schematic diagram of a layered medium

– The elements a_{ij} characteristic of smooth boundary conditions:
$a_{55} = 2s_2 \sinh S_2$, $a_{56} = -2 \cosh S_2$, $a_{57} = r_2 \cosh Q_2$, $a_{58} = -r_2 \sinh Q_2/q_2$.

New symbols which occur in the elements given above denote

$$\overline{S}_1 = -ks_1 z_1, \quad \overline{Q}_1 = -kq_1 z_1, \quad S_2 = -ks_2 z_1, \quad Q_2 = -kq_2 z_1,$$

where $z_1 = -h_2$ (see Fig. 1).

The quantities S_1 and Q_1 are defined by formulae (28), where $z_0 = -(h_1 + h_2)$.

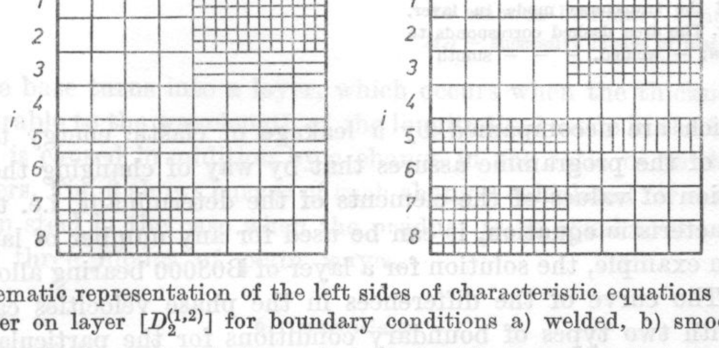

Fig. 2. A schematic representation of the left sides of characteristic equations in the case of layer on layer $[D_2^{(1,2)}]$ for boundary conditions a) welded, b) smooth

the crisscrossed area denotes zero elements, the area dashed horizontally denotes elements characteristic of welded conditions, the area dashed vertically corresponds to those of smooth conditions; the other elements are common

5. Results of numerical calculations

A numerical programme in Algol 1204 permits the phase velocities to be calculated for a given product of frequency and thickness of the superficial (first) layer, which product is the parameter of the calculations, in the case of welded and smooth boundary conditions; and the differences between these velocities to be determined for given modes of surface or plate waves. In the case of surface waves the calculations can be made only over the range of phase velocities lower than those of transverse waves in the base, thus corresponding to real elements [11, 12]. The complex elements involve the so-called "leaky

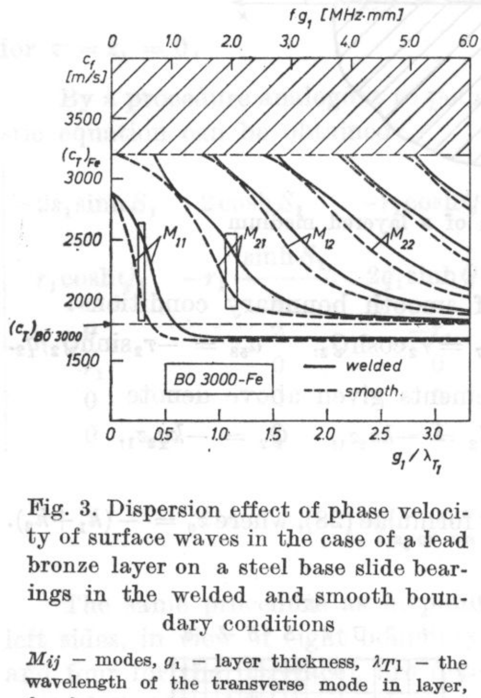

Fig. 3. Dispersion effect of phase velocity of surface waves in the case of a lead bronze layer on a steel base slide bearings in the welded and smooth boundary conditions

M_{ij} – modes, g_1 – layer thickness, λ_{T1} – the wavelength of the transverse mode in layer, f – frequency. The area dashed corresponds to leaky waves; – welded, – – – smoth

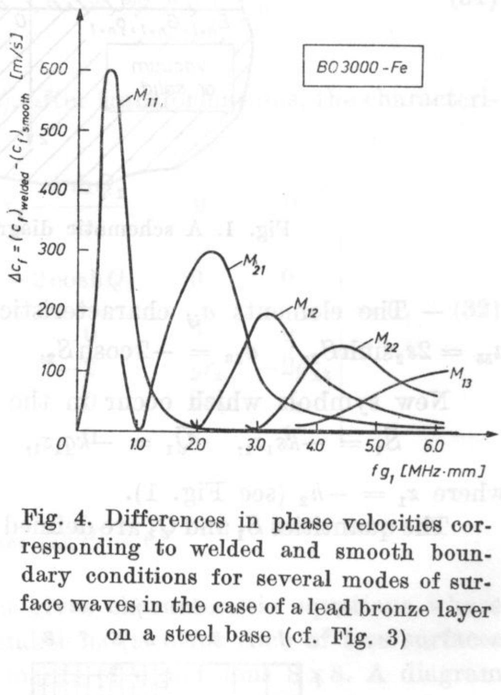

Fig. 4. Differences in phase velocities corresponding to welded and smooth boundary conditions for several modes of surface waves in the case of a lead bronze layer on a steel base (cf. Fig. 3)

waves" which are accompanied by a leakage of elastic energy to the base The design of the programme assures that by way of changing the procedure for calculation of values of the elements of the determinant, i.e. the left side of the characteristic equation, it can be used for any number of layers. Fig. 3 shows, as an example, the solution for a layer of B03000 bearing alloy on a steel base [13]. The curve of the differences in the phase velocities calculated ni this case with two types of boundary conditions for the particular modes of surface waves is shown in Fig. 4. From the point of view of the usefulness of velocity measurements for the estimation of adhesion degree it can be seen that there are optimum frequencies for a given layer thickness, i.e. those at which the differences in velocity are greatest. At the same time a further analysis shows that at those optimum frequencies the modes M_{11} and M_{21} are fairly sensitive to changes in layer thickness. For example, at frequency of 1 MHz a change in layer thickness by 0.05 mm causes a velocity change of 50 m/s (Fig. 5) in the case of the mode M_{11} in the welded boundary conditions.

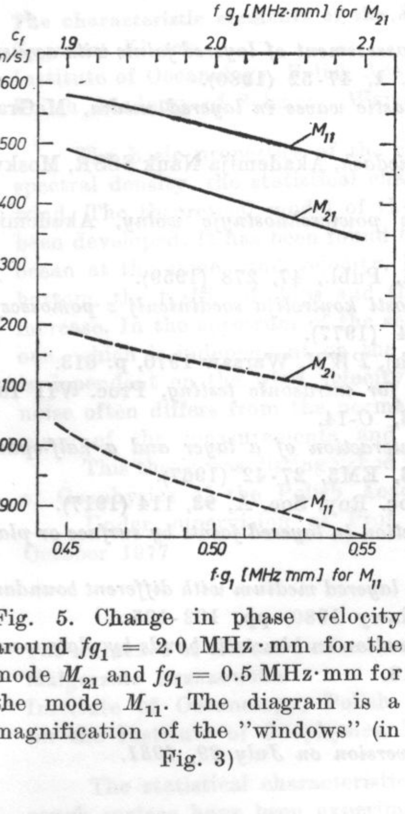

Fig. 5. Change in phase velocity around $fg_1 = 2.0$ MHz·mm for the mode M_{21} and $fg_1 = 0.5$ MHz·mm for the mode M_{11}. The diagram is a magnification of the "windows" (in Fig. 3)

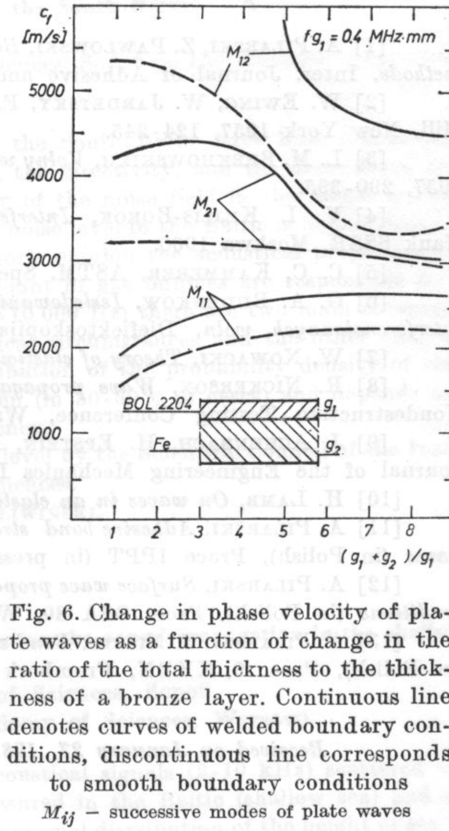

Fig. 6. Change in phase velocity of plate waves as a function of change in the ratio of the total thickness to the thickness of a bronze layer. Continuous line denotes curves of welded boundary conditions, discontinuous line corresponds to smooth boundary conditions
M_{ij} — successive modes of plate waves

When the base turns into a layer, which occurs when the thickness of the base is comparable to the wavelength of the longitudinal mode in the base, a velocity change is caused in addition by a change in the ratio of thicknesses of those two layers. Fig. 6 shows curves of such changes calculated for a BOL-2204 lead bronze on steel in the case when the product fg_1 is equal to 0.4 MHz·mm for the first three modes of plate waves.

6. Conclusions

Taking into consideration the practical possibilities of using the phase velocity measurements of surface or plate waves for the evaluation of adhesion degree (e.g. in bimetals), it can be stated that the knowledge of numerically determined dispersive curves for different boundary conditions facilitates a purposive selection of investigation parameters and permits the estimation of the effect on the quantity measured of such other factors as change in layer thickness or change in acoustic parameters characteristic of media connected.

References

[1] A. Pilarski, Z. Pawłowski, *Bond quality assessment of layered joints with acoustic methods*, Inter. Journal of Adhesive and Adhesion, **1**, 47-52 (1980).

[2] W. Ewing, W. Jardetsky, F. Press, *Elastic waves in layered media*, McGraw Hill, New York 1957, 124-245.

[3] L. M. Brekhowskikh, *Volny w sloistych sriedach*, Akademija Nauk SSSR, Moskva 1957, 290-395.

[4] V. I. Kejlis-Borok, *Interferentsionnyje powierchnostnyje wolny*, Akademija Nauk SSSR, Moskwa 1960.

[5] C. C. Kammerer, ASTM. Special. Techn. Publ., 47, 278 (1959).

[6] G. A. Budenkow, *Issledowanije wozmożnosti kontrolija soedinienij z pomoszczju interferencionnych woln*, Diefiektoskopija, **2**, 26-34 (1977).

[7] W. Nowacki, *Theory of elasticity* (in Polish), *PWN*, Warsaw 1970, p. 613.

[8] R. Nickerson, *Wave propagation theory for ultrasonic testing*, Proc. VII Int. Nondestructive Testing Conference, Warsaw 1973, *C*-14.

[9] J. Achenbach, H. Epstein, *Dynamic interaction of a layer and a half-space*, Journal of the Engineering Mechanics Division, **93**, EM5, 27-42 (1967).

[10] H. Lamb, *On waves in an elastic plate*, Proc. Roy. Soc. A, **93**, 114 (1917).

[11] A. Pilarski, *Adhesive bond strength evaluation in layered joints by surface or plate waves* (in Polish), Prace IPPT (in press).

[12] A. Pilarski, *Surface wave propagation in a layered medium with different boundary conditions* (in Polish), Proc. OSA 80, Warsaw—Puławy 1980, pp. 102-105.

[13] A. Pilarski, J. Niznik, *Bond strength evaluation in bimetalic bands by plate waves* (in Polish), Proc. 9 KKBN, Frombork 1979, *K*-18.

Received on January 27, 1981; revised version on July 29, 1981.

ABSTRACTS OF SOME DOCTORAL DISSERTATIONS IN POLAND

The characteristic elements of the sea noise in the South Baltic

Zygmunt Klusek
Institute of Oceanology, Polish Academy of Sciences, Sopot (in the Institute of Geophysics, Polish Academy of Sciences, Warsaw)

The basic properties of the sea noise in the South Baltic have been discussed: the spectral density, the statistical characteristics, the directivity, and the dependence on the wind. The theoretical model of the anisotropy of the noise field in the South Baltic has been developed. It has been found that the sea noise level in the Baltic is higher than in the ocean at the same wind velocity. In the author's opinion the acoustical properties of the bottom, the traffic of ships and the large amount of gas bubbles are responsible for this increase. In the spectrum of the sea noise (80 - 10 000 Hz) there are two main components: one, which is independent on the metereological circumstances and the other one, which is dependent on the wind velocity. The distribution of the probability density of the sea noise often differs from the normal distribution (in 30 - 50 % of cases) and depends on the place of the measurements and the frequency.

This thesis was distinguished for its high level by the Scientific Council of the Institute of Geophysics of the Polish Academy of Sciences.

Under supervision of Prof. Dr. A. Śliwiński.

October 1977

The influence of the sea surface and the bottom on the sound propagation in the shallow sea

Małgorzata Brzozowska
Institute of Oceanology, Polish Academy of Sciences, Sopot
(in the Institute of Geophysics, Polish Academy of Sciences, Warsaw)

The statistical characteristics of the acoustical signals (2 - 10 kHz) scattered on the rough surface have been experimentally measured in the Baltic (shallow sea) and in the Atlantic (deep sea). It has been found that the normal distribution of the height of sea waves and the scattered acoustical signals is satisfied in the deep sea but not in the shallow one. In the coastal zone the third and the fourth statistical moments of the described parameters must be taken into account and the normal distribution expanded into the Gram-Charlier series gives a good approximation for the distribution of the heights and the scattered acoustical signals. The coefficient of the sound reflection from the selected sediments of the Baltic sea has been measured by the interference method. The measurements have been performed in situ at frequencies from 2 to 10 kHz at normal incidence of the acoustic waves on the sea bottom. The theoretical model of the sound propagation with many reflections from the sea surface and the bottom has been discussed. The autocorrelation function of the scattered acoustical signals has been calculated as a function of the real distribution of the heights of surface waves and the coefficient of the bottom reflection.

This thesis was distinguished for its high level by the Scientific Council of the Institute of Geophysics of the Polish Academy of Sciences.

Under supervision of Prof. Dr. A. Śliwiński.

October 1977

Nonlinear effects in ultrasonic-laser light-diffraction

Marek Kosmol
Institute of Physics, University of Gdańsk

The aim of this paper was the experimental verification of the diffraction theory of high intensity laser beams on ultrasound propagating in liquids of nonlinear optical properties. This theory was developed by Józefowska, Śliwiński and the author of this paper. The experimental setup was designed and built. Some interesting problems were encountered in the design and construction of the experimental apparatus. The results which were obtained confirmed the theory under investigation, although the quantitative relations did not agree with predicted values. In addition to effects predicted theoretically a new effect was observed, i.e. selective extinction of light beams in the first orders of diffraction patterns. An attempt was made to explain this phenomenon.

Under supervision of Prof. Dr. A. Śliwiński.

September 1978

An analysis of pulsed ultrasonic transmit-receive systems for medical diagnostics

Anna Markiewicz
Institute of Physics, University of Gdańsk
(in the Institute of Fundamental Technical Research, Polish Academy of Sciences, Warsaw)

The paper presents a method for the calculation of the shape and size of pulses radiated and received by ultrasonic transmitting-receiving systems used in medical diagnostics. Using an equivalent electrical circuit for the transducer, the transfer functions for different working conditions of the transducer were calculated and, on the basis of these functions, the acoustical and electrical behaviour was calculated. By means of Laplace transformation output signals were computed for simple cases of open and shortcircuited electrical transducer terminals. Because of the complicated nature of the mathematical relations, a continuous Fourier transform (CFT) was used to describe the systems. This was then replaced by a discrete Fourier transform (DFT), thus preparing the relations for numerical calculations. The DFT was in turn calculated using the fast Fourier transform (FFT). Calculations were made for a number of practical cases. The paper also gives the results obtained from an analysis of the operation of a transmitting transducer for different types of acoustic matching, for a wedged transducer, and for a divided one.

This work was made possible by a grant from Polish Academy of Sciences, Institute of Fundamental Technological Research, Warsaw.

Under supervision of Prof. Dr. L. Filipczyński.

October 1978

Optical holographic method used in investigation of ultrasonic fields

Piotr Kwiek
Institute of Physics, University of Gdańsk

The aim of this paper was to describe theoretically and to verify experimentally the process of registration and reconstruction of holograms of ultrasonic fields. Three basic techniques used in optical holography, pulse double-exposured, average in time and real time, were considered. Experimental results obtained confirmed this theory. The experimental setup for investigation of ultrasonic fields was designed and the data obtained were computed by computer. This thesis was distinguished for its high level by the Council of the Faculty of Mathematics, Physics and Chemistry, University of Gdańsk and rewarded a prize by the Minister of Science, High Education and Technology.

Under supervision of Prof. Dr. A. Śliwiński.

June 1979

Acoustical relaxation in organic liquids of cyclic structure

Bogumił Linde
Institute of Physics, University of Gdańsk

Propagation of ultra- and hypersonic waves in organic cyclic liquids was investigated. The aim of this paper was to find compounds where acoustic Kneser relaxation occurs and to describe the relation between ultrasonic absorption caused by this process and molecular structure. On the basis of measurements and published standards of ultrasonic absorption for cyclic liquids some relations between $(a/f^2)_{\mathrm{rel}}$ and molecular structure were established. Acoustic Kneser dispersion could be observed in five compounds among 23 liquids examined. It was determined which internal vibrational degree of freedom took part in the process observed for two compounds.

Under supervision of Prof. Dr. A. Śliwiński.

June 1979

Holography — interferometric examination of vibrations of ultrasonic transducers radiating into liquids

Iwona Wojciechowska
Institute of Physics, University of Gdańsk

The aim of this study was to develop a suitable holographic method for detecting vibration amplitudes of ultrasonic transducers of the order of 10^{-9}m. A theoretical and experimental analysis of the holographic interferometry was performed. The optical holography with the phase modulated reference beam was chosen as the only suitable method for vizualization and quantitative examination of the vibration amplitude distributions of the ultrasonic transducers of the frequency 0.5-3 MHz radiating into a liquid. A progressive ultrasonic wave propagated in a transparent medium as an optical modulator with an optical filtering was used. The smallest value of the absolute amplitude detected with the procedure was of the order of 10^{-9}m. The vibration amplitude distribution throughout the surface of the transducers for various supplying and fixing conditions were presented.

This thesis was distinguished for its high level by the Council of the Faculty of Mathematics, Physics and Chemistry, University of Gdańsk and awarded a prize by the Minister of Science, High Education and Technology.

Under supervision of Prof. Dr. A. Śliwiński.

October 1979

Association of imidazole (1,3-diazole) and pyrazole in *p*-xylene examined with molecular acoustics methods

Mieczysław Jasiński
Institute of Physics University of Gdańsk

This paper contains results of examination of association of imidazole and pyrazole (hydrogen bonds) in non-polar solvent (*p*-xylene) and their interpretation based on ultrasonic velocity and attenuation of frequency 7.5 MHz for different concentrations 0.0-0.1% and temperatures 288-343 K. It has been shown that imidazole and pyrazole are good model compounds relating to acoustical properties. They increase the sound absorption of *p*-xylene solutions even at very small concentrations to a degree unnoticed so far in the literature. For the interpretation of results the theory of sound absorption applied in chemical reaction kinetics was developed and a comparison between the theory and experiment was performed, giving a good agreement. Different quantities which determine states of association of imidazole for different concentrations and temperatures were obtained.

Under supervision of Prof. Dr. A. Śliwiński.

October 1979

Impedance of the unbaffled semi-infinite cylindrical wave-guide

Anna Snakowska

Institute of Telecommunication and Acoustics, Technical University of Wrocław

The paper presents the phenomena occurring at the open end of a rigid wave-guide, assuming that only one of the allowed Bessel modes propagates towards the end. The solution of the wave equation at the suitable boundary conditions formulated by Wainstein shows that because of diffraction at the open end part of the wave energy is radiated outside and the remainder returns to the waveguide as a sum of the Bessel modes. In the paper the exact formulae of reflection and transformation coefficients as well as the outlet impedance for any order of incident wave are developed. The numerical calculations of moduli and the phases of reflection and transformation coefficients and also the real and imaginary part of impedance were made for the first six Bessel modes (including a plane wave) for a diffraction parameter in the range 0-20. Analysis of results obtained leads to the conclusion that the impedance of the outlet varies considerably for the different modes propagating towards the open end. Because of it the plane wave approximation, which is generally used, can lead to great errors in such a case when the participation of higher modes in the incident wave cannot be neglected.

Under supervision of Prof. Dr. Roman Wyrzykowski.

April 1980

Influence of crossover network and lay-out of loudspeakers in loudspeaker enclosure on the listening area

Krzysztof Rudno-Rudziński

Institute of Telecommunication and Acoustics, Technical University of Wrocław

The aim of this work is to find the listening area of a loudspeaker system, where the signal distortions occurring off the main axis of the system are not noticeable to the listener and to maximize this area. For these purposes the sound radiation by loud speaker systems was analysed in the context of a sort of the crossover network and the lay-out of loudspeakers on the cabinet front panel. Equations for directivity patterns of two-way loudspeaker systems with Butterworth filters in a crossover network were analysed. Power frequency response of the system was examined theoretically and experimentally. Formulae for intensity lateralization cues depending on the configuration of loudspeakers in both the enclosures belonging to a stereophonic sound system were obtained. The mathematical description of sound radiation by loudspeaker systems was used for the planning of psychoacoustic measurements. Psychometric curves of discriminability of the linear distortions versus time delay between signals coming to a listener from a woofer and a tweeter were measured. The measurements of intensity localization cues of stereophonic loudspeaker systems confirmed adequacy of the theoretical formulae. Knowing the type of a crossover network we can show a loudspeaker configuration which gives maximum spatial stability of sound images during the listening point displacement. Results of the theoretical considerations and the psychoacoustic measurements can be applied in the designing of the optimal lay-out of loudspeakers in monophonic and stereophonic systems. They allow us to determine the admissible mutual loudspeaker displacement on the front panel of a loudspeaker enclosure and in the depth of an enclosure.

Under supervision of Associate Prof. Janusz RENOWSKI.
February 1980

Application of linear prediction methods to linear system identification
Kazimierz Baściuk
Institute of Telecommunication and Acoustics, Technical University of Wrocław

In the dissertation the problem of linear system identification in the presence of disturbing quantization noise by means of linear predictive methods has been investigated. Among the three classical algorithms realizing linear prediction method, i.e. the Shanks, Steiglitz-McBride and Kalman algorithms, according to a reasonable assumption the last method has been chosen for further investigation. On the basis of the theoretical analysis of the problem and the results of experimental investigation, a criterion of choice of the quasioptimal model transfer function form $H(z)$, without disturbing noise, has been formulated. In the further part of the dissertation the estimation of the error of determination of coefficients of the model transfer function form $H(z)$ for disturbing noise, introduced by symmetrical quantizator, was derived, and the conception of a modified system of linear system identification based on the Kalman and Steiglitz-McBride methods was given. In the modified algorithm the failures of the applied methods were eliminated and their advantages used. In the modification the solution obtained by the Kalman method was treated as the exact one, and subsequently one iteration according to the Steiglitz-McBride algorithm was made. The criterion of choice of the quasioptimal solution in the linear system identification procedure has been formulated, i.e. quasioptimal form of the transfer function of the model of linear system identified, limiting our considerations to the case of identification in the presence of equidistant quantization noise, has been given. The threshold values of estimation of the error of identification of coefficients of the transfer function of systems investigated as well as the threshold values of energetic error have been given as a function of the number of bits. A series of experiments on the identification of a certain class of linear system has been carried out. In the dissertation the postulate of determination of the optimum criterion of choice of the model transfer function was neglected, and the quasioptimal criterion was used instead, thus simplifying greatly the method of determination of the choice solution indices. The results obtained in the experiments suggest the possibility of a practical application of the method to the identification of a wide class of minimumphase linear systems excitated by a unit impulse or minimumphase signals.

Under supervision of Associate Prof. Janusz ZALEWSKI.
March 1980

Analysis of frequency changes of transient state of sound propagating in a room
J. Lech Jugowar
Chair of Acoustics, Mickiewicz University, Poznań

The work comprises an analysis of the effect of momentary frequency changes of sound during its growth and decay process, depending on a series of selected acoustic parameters of the enclosure. Results indicate that momentary frequency changes of the transient state of sound propagating in a room have a character of smaller or larger fluctuations around a steady frequency value, and that the fluctuations for a specified direction of frequency changes can be relatively prolonged. The magnitude of momentary frequency changes depends on the growth or decay considered, on the time fragment of the investigated process, on the duration of sound sent to the enclosure, and on its frequency range. On the other hand, a strong dependence of the momentary frequency changes on the frequency response of the room, on the location of the measuring point, and to some extent on the reverberation conditions of the room has been observed. The work emphasizes the need for a psychoacoustic verification of the perception of the momentary frequency changes in sound, essential in the problem of the subjective evaluation of the room acoustic properties.

Under supervision of Associate Prof. Edward OZIMEK.

January 1981

THE SUMMER WORKSHOP ON THE INDENTIFICATION OF SOUND SOURCES AND THEIR PROPAGATION PATHS JABŁONNA 6-11 JULY, 1981

The Summer Workshop on the Identification of Sound Sources and their Propagation Paths was held at Jablonna on 6-11 July, 1981.

This Workshop was organized by the Committee on Acoustics of the Polish Academy of Sciences and Polish Acoustical Society in cooperation with the Institute of Fundamental Technological Research of the Polish Academy of Sciences and the Institute of Mechanics and Vibroacoustics of the Academy of Mining and Metallurgy, Cracow. The Workshop was sponsored by the International Institute of Noise Control Engineering. Prof. Stefan Czarnecki was the Chairman of the Workshop.

50 participants, including 20 foreigners from 10 countries, took part. Eleven two-hour lectures were delivered, eight of which were delivered by the foreign guests and three by Polish scholars. Each lecture was followed by round-table discussions.

The lectures and discussions were divided into the following sections:

I. Components of a single sound source – experimental methods.
II. Components of a single sound source – practical results.
III. Many sources – theory and calculation methods.
IV. Many sources – experimental methods.
V. Many sources – maesurement techniques.
VI. Many sources – practical results.
VII. Sound paths – experimental methods.

Ewa Kotarbińska (Warsaw)

THE JOVRNAL OF THE ACOVSTICAL SOCIETY OF JAPAN (*E*)

With real satisfaction we welcome the English version of periodical of the Acoustical Society of Japan, The Journal of the Acoustical Society of Japan (*E*).

Many of the papers in this periodical, which has appeared essentially in the Japanese language for many years, have been published in English. In addition the Editors have done much to bring the other papers closer to the international scientific community by publishing their abstracts, figure and table legends etc. in English. All these efforts have contributed to establishing a very good opinion of the investigations of Japanese acousticians and their Journal in the scientific world.

Nevertheless, in many cases, the language barrier has caused the periodical to contribute only partially to the international exchange of scientific information. This incomplete share of Japanese acousticians in this exchange was also felt by the Acoustical Society of Japan which, after analysis of the situation, decided to publish an English version of the journal of the Society each quarter of the year and to invite scientists in other countries to submit their papers to it, which will doubtless give the periodical a more international character.

Archives of Acoustics wishes every success to the Editorial Committee of the Journal of the Acoustical Society of Japan.

R. Gubrynowicz